DP-919

AEC RESEARCH AND DEVELOPMENT REPORT

MEASUREMENT OF MIGRATION AREA AND ANISOTROPY IN A MOCKUP OF THE EL-4 LATTICE

A. E. Dunklee
W. B. Rogers

DU PONT
REG. U. S. PAT. OFF.

Savannah River Laboratory

Aiken, South Carolina

Printed in USA. Price $3.00
Available from the Clearinghouse for Federal Scientific and Technical Information, National Bureau of Standards, U. S. Department of Commerce, Springfield, Virginia

664523

DP-919

Reactor Technology
(TID-4500, 35th Ed.)

MEASUREMENT OF MIGRATION AREA AND ANISOTROPY IN A MOCKUP OF THE EL-4 LATTICE

by

Albert E. Dunklee
Warren B. Rogers

Work done by

F. D. Benton
A. E. Dunklee
W. E. Graves
C. E. Jewell
G. F. O'Neill
W. B. Rogers
S. V. Topp
P. A. Lourme*

*Official observer representing Commissariat A L'Energie Atomique, Saclay, France.

Approved by

J. L. Crandall, Research Manager
Experimental Physics Division

November 1964

E. I. DU PONT DE NEMOURS & COMPANY
SAVANNAH RIVER LABORATORY
AIKEN, SOUTH CAROLINA

CONTRACT AT(07-2)-1 WITH THE
UNITED STATES ATOMIC ENERGY COMMISSION

ABSTRACT

Nuclear parameters of the lattice for the French power reactor, EL-4, were determined in mockup lattices at the Savannah River Laboratory. The reactor is to be D_2O moderated, gas cooled, and fueled with UO_2 rod bundles. The mockup lattice had a square lattice pitch of 23.09 cm and was fueled by 19-rod clusters of 1.27 cm diameter natural uranium rods inside air-filled 12.7-cm diameter housing tubes. Bucklings were determined for various pile shapes by measured flux profiles. Detailed studies were made of the diffusion properties of the lattice with emphasis on the anisotropic diffusion due to the neutron streaming in the air-filled channels. Such studies included determination of the axial migration area by neutron poisoning techniques as well as by observation of the neutron kinetics of the pile on stable positive periods. Ratios of axial to radial migration areas were deduced from the buckling measurements on the different shaped piles. Measurements of radial and axial diffusion coefficients were made by activation techniques and by measurements of the reactivity effect of introducing D_2O into coolant channels of selected pile positions. Agreement of the measurements with theoretical predictions was generally good.

CONTENTS

LIST OF TABLES

LIST OF FIGURES

MEASUREMENT OF MIGRATION AREA AND ANISOTROPY IN A MOCKUP OF THE EL-4 LATTICE

INTRODUCTION

As part of its program to develop nuclear power reactors, the Atomic Energy Commission of France (CEA) is building a large, D_2O-moderated, gas-cooled power reactor, the EL-4[1,2]. The EL-4 is almost identical in size with the Process Development Pile (PDP)[3] at Savannah River Laboratory, and the proposed EL-4 fuel assemblies are quite similar to some experimental fuel assemblies available at Savannah River. It thus appeared that the PDP might provide a ready made nuclear mockup of the EL-4 which could yield valuable information regarding the nuclear properties of gas-cooled lattices used in the EL-4.

A series of experiments was designed to take advantage of the SRL facilities in (a) providing a partial mockup of the EL-4 lattice and (b) obtaining general physics information on gas-cooled D_2O reactors. The principal areas of interest were the anisotropy and changes in migration area due to neutron streaming in the gas passages.

Two SRL facilities were proposed for these experiments; the Process Development Pile (PDP), and the Subcritical Experiment (SE)[4], the exponential facility at SRL. Table I compares some of the dimensions of the EL-4 lattice mockup in the PDP with the corresponding EL-4 dimensions.

TABLE I

Comparison of EL-4 Lattice Dimensions with PDP Mockup

Component	EL-4	PDP
Vessel diameter, cm	480	494
Fuel assembly	19 rods, natural and enriched UO_2	19 rods, natural UO_2
Fuel rod diameter, mm	11 or 13	12.7
Fuel housing tube diameter, cm	11.0	12.7
Lattice pitch (square), cm	23.0	23.09

SUMMARY

Under a contract between the French Atomic Energy Commission and the United States A. E. C., a set of experiments was performed at the Savannah River Laboratory in support of the EL-4, a French nuclear power reactor prototype under construction. The primary objectives of the experiments were to determine the migration area and the lattice anisotropy for a lattice similar to that proposed for the EL-4.

The migration area was determined by two methods; the poisoned moderator technique using copper tubes as the poison, and the period reactivity technique. A weighted average of 483 ±14 cm^2 was determined for $(L_z^2 + \tau_z)$ by the poisoned moderator technique; the period reactivity measurements gave a value of 492 ±11 cm^2.

Migration area anisotropy was determined by measuring the buckling of the lattice for three different core shapes in the critical facility (PDP), and for one core shape in the exponential facility (SE). The anisotropy, M_z^2/M_r^2, was 1.16 ±0.01 using the critical and exponential results together, and 1.13 ±0.03 using only the results of the critical measurements.

A method developed by Palmedo and Benoist for determining the radial diffusion coefficient of a lattice was applied to these experiments. The method presents an interesting approach to the study of the interaction of the microscopic and macroscopic fluxes and to the determination of the diffusion coefficient. The radial diffusion coefficient determined by this method agrees quite well with calculations.

A series of experiments using substitution techniques was applied toward obtaining the ratio of the vertical to radial diffusion coefficients. Although not entirely successful, the measurements provide useful information regarding the application of this method to voided lattices.

Data on the worth of the D_2O reflector were obtained for reflector thicknesses up to 125 cm. Because the EL-4 will be operated with a reflector, these data should aid in the evaluation of the reflector effectiveness.

DISCUSSION

FACILITIES AND LATTICES

Process Development Pile

The PDP[3] and its chief auxiliaries are illustrated in Figure 1. The reactor vessel is a bare, stainless steel tank with an inside diameter of 494 cm. Its effective height is controlled by the D_2O level and in these experiments was limited to 274 cm by the fuel assembly length. The mockup EL-4 fuel assemblies, described in a following section, were always loaded into the reactor on a square lattice pitch of 23.09 cm, center to center. Loadings were of several different sizes, ranging from 88 to 332 fuel assemblies, with various amounts of reflector. The loadings are shown in Figures 2 through 9 and are briefly described in Table II. The poison rod boundary in loading No. 6 (Figure 7) consisted of 2.54 cm diameter, aluminum-clad, Li-Al alloy rods, with a lithium concentration of 4.9 wt %. These rods were arranged on a 11.53 cm square pitch adjacent to the fuel and on a 23.09 cm square pitch in the outer region. The outer region in loading No. 7 (Figure 8) was poisoned with steel pipe assemblies 275 cm long on a 23.09 cm square pitch. These assemblies, illustrated in Figure 10, were selected to have approximately the same neutron diffusion and absorption properties as the fuel.

The moderator isotopic purity ranged from 99.57 to 99.54 mol % D_2O during the experiments; moderator temperature was 20 to 22°C.

TABLE II

Fuel Loadings in PDP

Loading No.	No. of Fuel Assemblies	Reflector*, cm	Remarks
1	332	10	Full pile load
2	332	10	Lattice poisoned with 156 copper tubes
3	332	10	Lattice poisoned with 301 copper tubes
4	216	50.4	Reflector unpoisoned
5	120	100.6	Reflector unpoisoned
6	120	~10	Thin reflector region. Outer region poisoned with Li-Al rods
7	156	None	Outer region poisoned with steel pipe assemblies
8	88	122	Reflector unpoisoned

* Refers to unpoisoned D_2O region between cylindricized radius of core and tank wall.

Subcritical Experiment and Standard Pile

An isometric view of the Subcritical Experiment (SE)[4] and its neutron source, the Standard Pile (SP)[5], is shown in Figure 11. The SE is an aluminum tank 153 cm in diameter and approximately 210 cm high. The tank wall is 0.953 cm thick and is covered on the outside by a cadmium sheet 0.16 cm thick. The tank rests on a graphite thermalizing column approximately 46 cm high and 153 cm in diameter. The SP is an enriched uranium reactor, graphite moderated, and H_2O cooled. The fuel and coolant are contained in an aluminum annulus approximately 46 cm in diameter, 10 cm thick, and 46 cm long located in the center of the 153 cm cube of graphite.

The two different loadings used in the SE measurements are shown in Figure 12. In both loadings the fuel assemblies were arranged at the 23.09 cm square lattice pitch. In one loading, however, a fuel assembly was centered in the SE tank (Figure 12A) while in the other an interstitial lattice point was centered in the tank (Figure 12B). These two loadings are designated fuel-centered and moderator-centered, respectively.

FUEL ASSEMBLIES

The fuel assemblies used in the measurements in the PDP are shown in Figure 13. They consisted of 19 uranium oxide rods arranged in hexagonally shaped clusters with 1.65 cm center-to-center rod spacing. The natural uranium oxide rods consisted of sintered UO_2 pellets 1.27 cm in diameter with a density of 10.4 g/cm^3 stacked in type 6063 aluminum tubes that were 1.39 cm OD by 0.051 cm thick. Rod spacing was maintained by small nylon rings at approximately 90 cm intervals along the rods. The rods consisted of a 91.6-cm-long top section joined to a 183.1-cm-long bottom section by a 1.04-cm-long aluminum connector. The 19 rod clusters were enclosed in 12.7-cm-OD by 0.145-cm-thick housing tubes of type 6063 aluminum. The clusters were centered in the housing tubes by means of 0.159-cm-thick spacers of type 1100 aluminum taped to the fuel assemblies near the bottom of the fuel assemblies and near the joint connecting the top and bottom rod sections. Calculations indicated that any changes in lattice buckling caused by these spacers or by the nylon-ring rod spacers were negligible. The housing tubes were provided with bottom plugs so that D_2O could be admitted to, or excluded from, the fuel. Details of the fuel location in relation to the bottom of the PDP are shown in Figure 14.

The fuel assemblies that were used in the SE were identical to those used in the PDP except that they were 183.1 cm long, consisting of the bottom section of fuel rods only.

BUCKLING MEASUREMENTS

PDP Buckling Measurements

Radial and vertical buckling measurements were made in four of the PDP loadings by measuring flux profiles in the critical lattices. The flux profiles were obtained by activating gold pins, 1.27 cm long by 0.016 cm diameter, in a large number of interstitial positions throughout the lattice. The gold pins were supported on the light aluminum rods shown in Figure 14. For vertical flux traverses the gold pins were spaced 10 cm apart in at least four different locations in the lattice. Radial flux traverses were obtained with at least 35 different radial locations using 3 different vertical levels at each location. A typical gold pin layout is shown in Figure 15.

In each irradiation run the critical moderator height was measured relative to an arbitrary zero point to within ±0.1 cm using a calibrated glass standpipe.

The irradiated gold pins were counted on NaI (Tl) scintillation counters biased to reject gammas of less than 300 kev. The count rates were corrected according to standard methods for background, dead time of the counters, and decay. Each set of gold pins was counted at least four times. The corrected count rates were then least squares fitted to J_o and cosine functions by an IBM 704 code, JOCOSE, to obtain the vertical and radial bucklings and their statistical errors. In the least squares fits, an attempt was made to eliminate errors due to boundary and reflector effects by running successive fits of the same sets of gold pin data and successively eliminating points from the extreme regions of the lattice. In all cases, the resulting bucklings showed only slight random variation as soon as the data taken near or at the extreme boundary were discarded. A typical vertical traverse is shown in Figure 16.

The combination of four or more countings of three or four traverses (radial and vertical, respectively) resulted in as many as 28 least squares fits in each loading. Except in cases where the counting was obviously bad due to instrument failure, the least squares results were simply averaged to obtain the geometrical bucklings for the lattice. The

averaged B^2 results for each lattice are given in Table III. The flag on these values represents the root mean square deviation of the several determinations in each lattice.

TABLE III

Results of Flux Mapping Irradiations and Data Fitting in PDP Loadings

Loading No.	Fuel Assemblies	No. of Fittings	Fitting Results, m^{-2} B_z^2	Fitting Results, m^{-2} B_r^2
1	332	28	2.361 ±0.011 (inner)(a)	0.852 ±0.008(b)
		10	2.285 ±0.013 (outer)	-
5	120 reflected	15	1.903 ±0.011	-
		18	-	1.255 ±0.008
6	120 lithium boundary	22	1.226 ±0.006	-
		11	-	2.039 ±0.011
7	156	27	1.516 ±0.005	-
		21	-	1.737 ±0.008

(a) Refers to vertical traverses taken over the baffle plate (inner) and away from the baffle plate (outer).

(b) The buckling result of the radial flux traverse in loading No. 1 was obtained from a one-region fit to a J_0 flux shape. It was not used in the final analysis for this loading. See page 15.

A number of corrections were applied to the vertical bucklings obtained from the flux traverses to obtain the clean lattice bucklings. These corrections are discussed below. No corrections were applied to the measured radial bucklings.

1. A correction was made to account for the poisoning effect of the flux mapping gold pins and their holders. This correction was determined experimentally by measuring the critical moderator height during the gold pin irradiation and again after the gold pin assemblies had been removed. The difference in moderator height between the two conditions was obtained with a precision of ±0.1 cm. It was assumed, as had been done in earlier work[6], that the difference between the extrapolated pile height, H, and the measured moderator height, S, was independent of the presence of the gold flux mapping assemblies in a given lattice. It was also assumed that the radial bucklings were unaffected by the gold.

Using these assumptions the measured change in critical moderator height obtained upon removing the gold was converted to a buckling correction. The accuracy of ±0.1 cm in measuring the moderator height change corresponds to an uncertainty of ±0.002 m^{-2} in buckling.

2. A correction was made to account for the presence of three air-filled thimbles used in all loadings as guide tubes for two control rods and a source rod. Three additional tubes, identical to the three already present, were inserted into the full loading (No. 1) in lattice positions equivalent to those of the first three tubes. The resulting change in buckling was used directly as the correction for this loading. The corrections for the rest of the loadings were calculated from the measured number for loading No. 1 using the relative statistical weights of the tubes in each loading. The corrections ranged from 0.003 to 0.006 m^{-2}. An uncertainty of ±0.001 m^{-2} was assigned to them.

3. The temperature and D_2O purity changed slightly during the experiments necessitating small corrections to put all bucklings on the same basis. The temperature and D_2O purity coefficients of reactivity were calculated using the BSQ code[7], an IBM 704 code routinely used at SRL to calculate heavy water lattices. The coefficients were 0.01 $m^{-2}/°C$ and 0.62 $m^{-2}/\%$ D_2O, respectively. All buckling measurements were corrected to 20°C and 99.57 mol % D_2O. Temperature and D_2O purity changes were measured with precisions of ±0.003°C and ±0.005% D_2O, respectively, so that the uncertainty on the correction factor is negligible. However, the absolute temperature uncertainty was about ±0.5° and the uncertainty in absolute D_2O purity was ±0.02% D_2O resulting in absolute buckling uncertainties of ±0.005 m^{-2} and ±0.012 m^{-2}, respectively.

4. A final correction was applied to account for the decrease in buckling due to the gap in the fuel at the connection between the top and bottom fuel sections. This correction was obtained by a flux measurement across the gap to determine the effect on f and L^2 together with calculations to determine the effect on p. This calculation is fully described on page 36. An uncertainty of ±25% was assigned to this correction.

The corrections and the final bucklings for all loadings are summarized in Table IV. The uncertainties discussed above were statistically combined to give the flags for the first four loadings in Table IV.

The bucklings for the last four loadings listed in Table IV were not measured by flux mapping, but were obtained from the critical moderator heights measured in these loadings. In each of the flux-mapped loadings (No. 1, 5, 6, and 7), 17.4 cm was the difference between the critical moderator height, S, measured with the glass standpipe, and the extrapolated pile height, H, obtained from the gold-count-rate data. This result confirms earlier indications[6] that the quantity H minus S is independent of the pile height for a given lattice. The vertical bucklings for loadings No. 2, 3, 4, and 8 in Table IV were therefore obtained simply by adding 17.4 cm to the measured moderator height to obtain the extrapolated pile height.

The radial bucklings for loadings No. 2 and 3 were assumed to remain unchanged from loading No. 1 because the only change made in the lattice was the addition of copper poison tubes. For loadings No. 4 and 8 in which no direct measure of the radial buckling was obtained, use was made of the relationship

$$\frac{B_{r_2}^2 - B_{r_1}^2}{B_{z_1}^2 - B_{z_2}^2} = \frac{M_z^2}{M_r^2} . \qquad (1)$$

$\frac{M_z^2}{M_r^2}$, is the lattice anisotropy discussed on page 18, and

$B_{r_1}^2$, $B_{z_1}^2$, $B_{r_2}^2$, and $B_{z_2}^2$ refer to geometrical bucklings in two differently shaped loadings (eg, different numbers of fuel assemblies) of the same lattice. Using the value 1.16 for the lattice anisotropy (see page 19) together with the vertical bucklings discussed above, the radial bucklings given in Table IV for loadings No. 4 and 8 were computed by equation (1).

TABLE IV

Summary of Measured Bucklings and Corrections in PDP Loadings

Loading No.	Corrections, m^{-2}: Flux Detector Poisoning	Guide Tubes	Temp to 20°C	D_2O to 99.57 mol %	Fuel Gap	Final Bucklings, m^{-2}: B_z^2	B_r^2
1	+0.039	+0.003	+0.008	+0.002	0	2.413 ±0.018	0.826 ±0.015
5	+0.065	+0.005	+0.009	+0.006	+0.005	1.993 ±0.018	1.255 ±0.008
6	+0.078	+0.006	+0.006	+0.008	+0.010	1.334 ±0.016	2.039 ±0.011
7	+0.068	+0.006	+0.018	+0.017	+0.007	1.632 ±0.015	1.737 ±0.008
2						2.03 ±0.03	0.83 ±0.02
3						1.64 ±0.02	0.83 ±0.02
4						2.35 ±0.03	0.86 ±0.05
8						1.64 ±0.02	1.62 ±0.04

A unique situation was presented by the full pile loadings of 332 fuel assemblies which extended out beyond the moderator inlet baffle plate shown in Figure 15. This plate, which is 1.27-cm-thick stainless steel, is located 3.81 cm above the nominal tank bottom and effectively divides the pile into two radial regions with a small difference in vertical buckling between them. The effect is clearly shown in the vertical flux traverse results listed in Table V for loading No. 1.

To determine a more nearly correct lattice buckling for this loading, an IBM 704 code was written to make a least squares fit of the radial traverse data to a two region solution of the one group diffusion equation. The form to which the data were fitted was

$$\phi(r) = AJ_o (B_r r), \quad r<R_o$$

$$\phi(r) = CJ_o (B'_r r) + C'Y_o (B'_r r), \quad r>R_o \qquad (2)$$

where R_o is the cylindricized radius of the baffle plate (108 cm) and B_r and A are the fitting parameters (C and C' are determined as functions of A by continuity of flux and current at R_o).

Figure 17 shows the results of fitting the radial flux traverse data for loading No. 1 with various values of

$$\Delta B_r^2 = B_r^2 \text{ outer} - B_r^2 \text{ inner} \qquad (3)$$

To arrive at the proper value of ΔB_r^2, it was assumed that the difference in vertical buckling between the two regions as measured in the vertical flux traverses was equal, after correction for anisotropy, to the difference in radial buckling in the two regions. The vertical buckling difference was measured as 0.078 m^{-2} (Table V) and the lattice anisotropy was determined as 1.16 (see page 19). Therefore, the ΔB_r^2 is 0.078 x 1.16 = 0.09 m^{-2}, and from Figure 17 the radial buckling of the inner region is 0.826 m^{-2}. The required bucklings are:

$$B_r^2 = 0.826 \text{ m}^{-2} \text{ (inner)}$$

$$B_z^2 = 2.413 \text{ m}^{-2} \text{ (inner)}$$

These values are listed in Table IV.

TABLE V

Vertical Flux Traverse Results in PDP Loading No. 1

Traverse Rod[a]		Fitting Results B_z^2, m^{-2} Individual Traverses, Uncorrected Results	Averaged Corrected Results
A	Over	2.364	2.413
B	Baffle	2.367	
C	Plate	2.345	
D		2.363	
E	Away from	2.283	2.335
F	Baffle Plate	2.286	

(a) Refers to vertical traverse rod locations in loading. See Figure 15.

SE Buckling Measurements

In the SE experiments, the vertical buckling, κ_z^2, is determined from the vertical flux distribution as measured by a small, movable ion chamber. Because there are fast neutrons leaking into the SE along with the thermal neutron source, and also because of the photoneutrons created by SP gamma rays reaching the SE, it is necessary to make a background flux determination with each measurement. The background run is made with a cadmium sheet between the SE and the SP. The net flux distribution – the difference between the total and background fluxes – is then fitted by the method of least squares to the function

$$\Phi_1 = A \sinh \kappa_z (X + \delta - Z_1) \qquad (4)$$

where Φ_1 = the flux measured at some vertical position, Z_1;

A = a constant;

κ_z^2 = (vertical relaxation length)$^{-2}$;

X = distance from the top surface of water to some zero point from which Z_1 is measured; and

δ = vertical extrapolation length.

Initially, the data are fitted to the above expression, assuming A, κ_z, and δ as unknown. The least squares fitting of the data is not sensitive enough to allow the best values of all three parameters to be determined from each measurement; therefore, an average value of δ is determined from

three parameter fits for all data on all lattices; then the data are refitted to the parameters A and κ_z.

For the SE lattice arrangements shown in Figure 12, three different measurements of κ_z^2 were made in the unpoisoned lattices — one measurement preceding the insertion of copper poison tubes in the lattice and two following the removal of the tubes. Each measurement consisted of from 4 to 8 separate traveling monitor traverses. Measurements with the poison tubes in place consisted of 10 and 4 determinations of κ_z^2 for the fuel-centered and moderator-centered lattices, respectively. The maximum spread in κ_z^2 between the separate traverses in a single measurement was ± 0.02 m^{-2}.

Using the calculated D_2O purity coefficient of 0.62 m^{-2}/% D_2O, the measured κ_z^2 values were corrected to a reference D_2O purity of 99.57 mol % D_2O. Table VI lists the final κ_z^2 values obtained for the SE lattices.

TABLE VI

κ_z^2 Measurements in the SE

Lattice	κ_z^2, m^{-2} Clean	Copper
Moderator-centered[a]	4.64	5.35
Fuel-centered[a]	4.60	5.37

(a) Each point assigned an uncertainty of ± 0.03 m^{-2}.

Radial buckling measurements were made in each of the lattice arrangements shown in Figure 12. Five levels of gold pins, 7.6 cm apart, were placed in the positions indicated. For reasons discussed on page 16, it was necessary to repeat each irradiation with the cadmium sheet between the SE and the SP. The net activities were fitted to the expression

$$\phi_1 = AJ_o(B_r r_1). \qquad (5)$$

Table VII lists, for each lattice arrangement, the resulting values of B_r^2, a mean value, and the standard deviation of the mean.

TABLE VII

Radial Buckling Measurements in the SE

Level	B_r^2, m^{-2} Moderator-Centered	Fuel-Centered
1 (bottom)	9.04	8.96
2	9.01	9.01
3	9.06	8.91
4	9.10	8.93
5 (top)	9.06	8.88
Mean	9.05 ±0.02	8.94 ±0.03

Results of previous experiments lead to the belief that the true uncertainty is not represented by the standard deviations listed in the table and that ±0.05 m^{-2} is more realistic. The difference measured between the two lattice loadings is real, because the fuel-centered lattice has a thicker reflector than the moderator-centered lattice.

ANISOTROPY DETERMINATION

In reactor lattices that contain voids, the critical geometrical buckling, $(B_r^2 + B_z^2)$, is not characterized by the lattice parameters alone, but depends on the geometry of the system. This results from the fact that the directional components of the migration area are unequal because of voids in the lattice. In one-group notation

$$k_\infty - 1 = M_r^2 B_r^2 + M_z^2 B_z^2 \qquad (6)$$

which may be rewritten as

$$(B_r^2 + B_z^2) = \frac{k_\infty - 1}{M_r^2} - \frac{M_z^2 - M_r^2}{M_r^2} B_z^2 \qquad (7)$$

Therefore, the critical geometrical buckling, $(B_r^2 + B_z^2)$, for any particular lattice shape, is a linear function of the vertical buckling. The anisotropy, M_z^2/M_r^2, may be determined from critical buckling measurements made in at least two different geometrical shapes by determining the slope, $(M_z^2 - M_r^2)/M_r^2$, of the line passing through a plot of $(B_r^2 + B_z^2)$ versus B_z^2.

In the present experiment, cores of five different shapes were used, including the subcritical cores in the SE. These cores were loading No. 1, 6, and 7 in the PDP and the two SE loadings.

The buckling results for these lattices are plotted in Figure 18. Only reduced cores with a "poisoned" reflector and full pile loadings were used in establishing the slope of the line. The least squares fit to the data using both SE and PDP points yields

$$\frac{M_z^2 - M_r^2}{M_r^2} = 0.16 \text{ or, } \frac{M_z^2}{M_r^2} = 1.16 \pm 0.01.$$

Using only the PDP data points yields 1.13 ±0.03 for the anisotropy. The uncertainty indicated for these two values represents the standard deviation of the least squares fit of the experimental points (five and three points, respectively).

The theory of Benoist[8,9] was used to obtain a theoretical value of the anisotropy. The two group parameters used as input in the calculation are given in Table VIII. The calculation gave a value of 1.17 for M_z^2/M_r^2, in very good agreement with the measured result.

TABLE VIII

Input Parameters for Calculation of Migration Area Anisotropy

Parameter	Value
Average thermal flux in moderator region (arbitrary units)	134.08
Average thermal flux in fuel region	87.40
Outer radius of fuel, cm	3.761
Outer radius of void region, cm	6.35
Lattice pitch, cm	23.09
Thermal transport mean free path in moderator region, cm	2.478
Thermal transport mean free path in fuel regions, cm	4.735
Fast transport mean free path in moderator regions, cm	3.46
Fast transport mean free path in fuel region, cm	5.085
Ratio of thermal flux at fuel surface to average flux in fuel[a]	1.170
Thermal macroscopic absorption cross sections in fuel region[a], cm^{-1}	0.08355
Fermi age for moderator (99.6 mol % D_2O), cm^2	128.4
Effective thermal, macroscopic absorption cross sections in cell, cm^{-1}	0.0552

NOTE: Thermal cross sections and flux ratios were obtained from THERMOS calculations[11]

(a) These parameters were used to calculate the average thermal flux in the void region.

VERTICAL MIGRATION AREA

Copper Poison Method

One method of determining the migration area of a lattice is to add a known amount of absorber uniformly to the lattice (thereby introducing a change in k_∞) and then measure the resulting change in critical buckling. If the two-group, anisotropic form of the critical equation is used,

$$k_\infty = \eta\epsilon pf = (1 + L_r^2 B_r^2 + L_z^2 B_z^2)(1 + \tau_r B_r^2 + \tau_z B_z^2) \quad (8)$$

it can be shown that

$$(L_z^2+\tau_z) = \frac{\frac{\Delta f}{f}\left[1+L_z^2(GB_r^2+B_z^2+\Delta B_z^2) - 2L_z^2\tau_z\Delta B_z^2(GB_r^2+\Delta B_z^2)\right]}{\Delta B_z^2 - (GB_r^2+B_z^2)(\frac{\Delta f}{f} + \frac{\Delta p}{p})}$$

$$+ \frac{\frac{\Delta p}{p}\left[1+L_z^2\tau_z(GB_r^2+B_z^2)^2\right] - L_z^2\tau_z\left[(2GB_r^2+B_z^2)\Delta B_z^2+(\Delta B_z^2)^2\right]}{\Delta B_z^2 - (GB_r^2+B_z^2)(\frac{\Delta f}{f} + \frac{\Delta p}{p})} \quad (9)$$

It is here assumed that the only terms affected by the addition of the absorber are f, the thermal utilization; p, the resonance escape probability; and L^2, the thermal diffusion area. All of the terms in (9) have their standard definitions except for G, which is equal to M_r^2/M_z^2, and which was inserted to allow τ_r and L_r^2 to be expressed in terms of τ_z and L_z^2, respectively. Assuming that τ and L^2 have the same G term has negligible affect on the results.

In the present experiments, the absorbing poison was copper tubes, 1.588 cm outside diameter with a 0.069 cm nominal wall thickness. These tubes were added to several lattices and the resulting changes in vertical buckling, B_z^2, were measured. These lattices were: (1) 332 fuel assemblies, PDP, copper in alternate positions in the pile, Figure 3; (2) 332 fuel assemblies, PDP, copper in all possible positions, Figure 4; (3) 32 assemblies, SE, copper in all possible positions, Figure 12B; and (4) 29 assemblies, SE, copper in all possible positions, Figure 12A. The copper tubes were placed at the corners of the square lattice cells. The dimensions of 50 of the 300 copper tubes were measured; cross-sectional area varied by no more than about ±1%, from an average value of 0.3265 cm^2. Chemical and spectrographic analyses of a representative sample of the copper revealed no appreciable quantities of other absorbing materials.

The absorption ratio between the copper tubes and the fuel was measured in lattices (1) and (2) above, and later in a special loading in which the center 40 positions of a 156-assembly pile in the PDP contained copper tubes. Machined copper foils, 1.27 cm in diameter and 0.015 cm thick, were placed between fuel pellets in each of the four rod symmetry types in the test fuel assemblies. In each irradiation, four vertical levels of bare foils and one level of cadmium-covered foils were used. Foils 1.27 cm in diameter and 0.015 cm thick were cut from two of the copper tubes at levels corresponding to the measurement levels in the fuel. Epicadmium activities in the copper tubes were determined by placing copper strips, 1.27 cm long, 0.015 cm thick, and 0.15 cm wide, in 0.076-cm-thick cadmium wrappers at the surface of the copper tubes. All foils were counted several times with scintillation counters. Foils were calibrated by irradiation in a uniform thermal flux.

The ratios of the average neutron density in the copper tubes to the average neutron density in the fuel obtained from the corrected foil count rates in each lattice are given in Table IX. The headings Cu_1 and Cu_2 refer to the two copper tubes from which foils were cut following the irradiation.

TABLE IX

Ratio of Average Neutron Density in Copper Tubes to Average Neutron Density in Fuel, as Measured by Copper Foils

Loading	$\bar{n}_{Cu_1}/\bar{n}_U$	$\bar{n}_{Cu_2}/\bar{n}_U$
1/2 copper loading, lattice (1)	1.757	1.732
Full copper loading, lattice (2)	1.667[(a)]	1.766
Special loading	1.749	1.749
Average and standard deviation of average	1.751 ±0.005	

(a) The value of 1.667 was omitted from the average since it differs from the mean by more than 3σ.

The ratio of absorptions within one fuel assembly to absorptions within one copper tube is obtained from the above ratios by:

$$\frac{(\Sigma_a \phi V)_{Cu}}{(\Sigma_a \phi V)_U} = \frac{(\bar{v}\bar{\Sigma}_a \bar{n} V)_{Cu}}{(\bar{v}\bar{\Sigma}_a \bar{n} V)_U} = \frac{\bar{n}_{Cu}}{\bar{n}_U} \cdot \frac{V_{Cu}}{V_U} \cdot \frac{(\bar{v}\bar{\Sigma}_a)_{Cu}}{(\bar{v}\bar{\Sigma}_a)_U} \qquad (10)$$

The ratio of the effective cross sections times the average velocity within the fuel was determined from a THERMOS[11] calculation to be 1.8716. Assuming the uranium oxide rods to be exactly 1.27 cm in diameter, the volume ratio was determined from measured weights of the copper tubes to be 0.01356 ±1%. Thus, the absorption ratio between fuel and copper tubes is

$$\frac{(\Sigma_a \phi V)_{Cu}}{(\Sigma_a \phi V)_U} = (1.751)(1.8716)(0.01356) = 0.04445$$

In a finite lattice there are unequal numbers of fuel assemblies and copper tubes and they are not in a flat flux; therefore it is necessary to flux-weight the copper and fuel absorptions. The flux-weighting ratio, designated Q, is given by

$$Q = \frac{\sum_i N_i J_o (Br_i)}{\sum_j N_j J_o (Br_j)} \qquad (11)$$

where the subscript i refers to copper tubes and j to fuel assemblies.

The flux weightings for each of the lattices measured are given in Table X.

TABLE X

Flux-Weighting Copper Tubes and Fuel Assemblies

Lattice	Q
SE, moderator-centered	0.8515
SE, fuel-centered	0.9363
PDP, 1/2 copper loading	0.4704
PDP, full copper loading	0.9301

In equation (9) the measured quantities are $\Delta f/f$, B_r^2, B_z^2, ΔB_z^2, and G. The remaining quantities are calculated. The procedures for measuring B_r^2, B_z^2, ΔB_z^2, and G were described previously in this report. The method of obtaining $\Delta f/f$ from the measured copper absorptions and the method for calculating $\Delta p/p$ are in the following sections, along with the final $(L_z^2 + \tau_z)$ values.

Δf/f Determination

For purposes of development, define

f = thermal utilization, infinite lattice, no poison

f' = thermal utilization, infinite lattice, poisoned (12)

f'' = thermal utilization, finite lattice, poisoned

then,

$$\frac{1}{f} = \frac{\text{absorptions in cell}}{\text{absorptions in fuel}} \tag{13}$$

$$\frac{1}{f'} = \frac{1}{f} + \left(\frac{\text{absorptions in 1 poison tube}}{\text{absorptions in 1 fuel assembly}}\right)_{\text{flat } \phi} \cdot R \tag{14}$$

where $R = \left(\frac{\text{number of poison tubes}}{\text{number of fuel assemblies}}\right)_{\text{infinite lattice}}$

$$\frac{1}{f''} = \frac{1}{f'}\,(Q) \tag{15}$$

where Q is the flux-weighting ratio of the poison tube positions with respect to the fuel positions given in Table X.

Essentially, the Δf/f determination consists of evaluating equation (15) using a calculated value of f.

Using equation (14), equation (15) may be written:

$$\frac{1}{f''} = \frac{1}{f} + \frac{(\phi\Sigma_a V)_{Cu}}{(\phi\Sigma_a V)_U}\,(Q) \tag{15a}$$

This equation is then used to determine f''. The evaluations of (15a) are given in Table XI together with the resulting values of Δf/f.

TABLE XI

Δf/f due to Addition of Copper Tubes to Lattice

Lattice	f''	Δf/f
SE, moderator-centered	0.91233	0.03443
SE, fuel-centered	.90917	.03777
PDP, 1/2 copper poison	.92661	.01932
PDP, full copper poison	0.90942	0.03751

Δp/p Calculation

The resonance neutron capture in the lattice containing copper tubes is increased by the resonance capture in Cu^{63} and Cu^{65} and by the epicadmium 1/v absorptions. The equations for resonance capture can be approximated by

$$\text{Resonance capture} = (1-p) = \frac{N_U}{\xi\Sigma_s^{D_2O}} \frac{V_U}{V_m} RI^U \qquad (16)$$

$$(1-p') = (1-p) + \frac{N_{Cu}}{\xi\Sigma_s^{D_2O}} \frac{V_{Cu}}{V_m} \left[\chi RI^{Cu^{63}} + (1-\chi)RI^{Cu^{65}} + \sigma_{1/v}^{Cu}\right] \qquad (17)$$

$$(1-p'') = (1-p')(Q) \qquad (18)$$

$$(p'' - p) = - \frac{N_{Cu}}{\xi\Sigma^{D_2O}} \frac{V_{Cu}}{V_m} \left[\chi RI^{Cu^{63}} + (1-\chi)RI^{Cu^{65}} + \sigma_{1/v}^{Cu}\right] (Q) \qquad (19)$$

where N = number of atoms per unit volume

$\xi\Sigma_s^{D_2O}$ = slowing down power of moderator

χ = isotopic abundance of Cu^{63}

$(1-\chi)$ = isotopic abundance of Cu^{65}

RI = resonance integral

Q = flux-weighting ratio poison positions with respect to fuel positions defined previously.

Then,

$$\frac{\Delta p}{p} = \frac{p'' - p}{p} \qquad (20)$$

In equations (16) through (20), the primes have the same definitions as those used in discussing Δf/f.

Values of Δp/p were calculated using equations (19) and (20), together with the weighting terms given in Table X and the following parameters.

$$\xi\Sigma_s^{D_2O} = 0.186 \text{ cm}^{-1}$$

$$\frac{V_{Cu}}{V_U} = 8.033 \times 10^{-4}$$

$$RI^{Cu^{63}} = 1.4 \text{ barns (for 0.069 cm thickness)}^{(12)}$$

$$RI^{Cu^{65}} = 1.1 \text{ barns}$$

$$\sigma_{1/v}^{Cu} = 1.83 \text{ barns}$$

$$\frac{\Delta p}{p} = (1.52 \times 10^{-3})\ (Q)$$

The values of $\Delta p/p$ for each lattice are listed in Table XII.

Results

The parameters used to evaluate equation (9) for $(L_z^2-\tau_z)$ are summarized in Table XII together with the resulting values of M_z^2.

TABLE XII

$(L_z^2+\tau_z)$ from Copper Poisoning Method

Lattice	$\Delta f/f$[b]	$\Delta p/p$[c]	B_r^2, m^{-2}	B_z^2[a], m^{-2}	B_z^2, m^{-2}	$(L_z^2+\tau_z)$, cm^2
SE, mod-cen	3.443	1.29	9.05	-4.64	0.71	474 ±30
SE, fuel-cen	3.777	1.42	8.94	-4.60	0.77	481 ±30
PDP, 1/2 Cu	1.932	0.72	0.83	2.41	0.382	510 ±15
PDP, full Cu	3.751	1.41	0.83	2.41	0.770	476 ±11
					Average	483 ±14

(a) Clean buckling, no copper.
(b) Multiply x 10^{-2}.
(c) Multiply x 10^{-3}.

The other quantities needed to evaluate equation (9) are the value of $G = M_r^2/M_z^2$, which was taken from the experiments as 1/1.16, and trial values of L_z^2 and τ_z. These latter quantities were obtained from Benoist-type calculations[8,9], using the data listed in Table VIII. The calculations gave $L_z^2 = 286.4$ cm^2 and $\tau_z = 240.7$ cm^2.

Iterating new values of L_z^2 and τ_z into equation (9) had negligible effect on the results.

The errors indicated on each value of M_z^2 in Table XII represent the experimental errors in $\Delta f/f$ and in ΔB_z^2. The standard deviation of ±0.3% in the measured absorption ratio propagates through to $\Delta f/f$. ΔB_z^2 was measured to ±0.005 m^{-2} in the PDP or to ±1.5% in the 1/2 copper loading and to ±0.7% in the full copper loading. In the SE, B_z^2 can be measured to ±0.02 m^{-2} so that the error in ΔB_z^2 = ±0.03 m^{-2} or ±4.0%. Another source of systematic error in $(L_z^2+\tau_z)$ comes from the uncertainty of approximately ±1% in the ratio of absorption cross sections for copper and uranium. This ±1% uncertainty propagates through $\Delta f/f$ to $(L_z^2+\tau_z)$ as a ±5 cm^2 systematic error in all measurements. The average value of 483 ±14 cm^2 includes all sources of uncertainty listed above.

Period Method

A second independent determination of the migration area of the EL-4 mockup lattice was obtained by period measurements. In this method, the vertical geometrical buckling of the critical lattice is decreased a known amount and the resulting positive period is measured. A calculated period reactivity relationship is then used to obtain Δk_{eff}. By means of two group theory $(L_z^2+\tau_z)$ is then calculated from the values of $\Delta k_{eff}/\Delta B_z^2$.

The first step in the experimental procedure was to reach a stable pile power and measure the critical moderator height of the clean lattice with no control rods present. At this stage the absolute pile power was relatively low (~50 watts), but the signal from the flux measuring instruments was about 3 orders of magnitude above that at initial startup. The moderator height was then slowly increased by some predetermined amount, usually about 1½ to 2 cm, while the pile power was held constant by inserting control rods. The new moderator height was measured. Next the control rods were rapidly driven out of the pile with the moderator height held constant. During the increase in pile power the flux level was monitored by four to six compensated ion chambers and two BF_3 counting systems. The currents from the compensated ion chambers were recorded on strip-chart recorders as a function of time, and the BF_3 counts were tabulated at fixed time intervals. The pile power was allowed to increase two or three orders of magnitude at which time the power was leveled off by dropping moderator back to its initial height. After about 20 minutes of constant power operation at the higher level, the moderator height was again measured and the pile shut down.

Period measurements were made six times in each of two different loadings, a total of twelve critical runs. The difference in moderator height between the critical and supercritical conditions, and the pile period was obtained from each measurement.

The moderator height difference, ΔH, was measured with an electrical probe capable of determining relative water heights with a precision of ±0.005 cm. The critical moderator heights determined at the higher power level were used in the calculations thus ensuring that any photoneutrons resulting from gamma activity from previous runs would be negligible in comparison to the fission neutrons. From the measured ΔH value the change in vertical buckling was calculated for each run.

The pile period for each run was calculated using the flux data obtained from the compensated ion chambers and BF_3 counting systems. The flux data during the initial part of the flux rise were not used in calculating the period; the waiting period was calculated to allow the pile period to reach its asymptotic value within 1%.

The measured ΔH values and doubling times, along with the calculated ΔB_z^2 values, are given in Table XIII. The uncertainties on the doubling times are the root-mean-square deviations obtained from the several instruments in each run. The nominal uncertainty in subsequent calculations is taken as ±1 sec. The uncertainties in ΔB_z^2 result from the allowances of ±0.01 cm in the measured ΔH and of ±0.2 to 0.5 cm in the absolute pile heights.

Values of Δk_{eff} corresponding to the measured periods were obtained from a calculated period reactivity relationship. The delayed neutron and photoneutron groups were based on the neutron data given by Keepin[18].

Other constants used in the calculation were the average numbers of neutrons per fission $\nu^{28} = 2.80$, $\nu^{25} = 2.42$, and the neutron lifetime, $\ell = 3.3 \times 10^{-4}$ sec. Two additional parameters used in the calculations were δ, the ratio of U^{238} to U^{235} fissions; and T, the fraction of high energy gamma rays escaping capture or degradation in the fuel. These parameters depend upon the fuel assembly only and were calculated for this experiment as $\delta = 0.0427$ and $T = 0.39$. It is quite possible that the value of δ used in this calculation was in error by 5 to 10%. The value of T possibly was in error by as much as 10%. The sensitivity of the results to changes in these parameters is given in Table XIV.

The calculated values of Δk_{eff} are given in Table XIII. Also given in this table is the quantity $(\Delta k_{eff}/-\Delta B_z^2)$, which should be a constant for this experiment.

TABLE XIII

Period Measurements in PDP

Loading No.	Run	ΔH, cm	$-\Delta B_z^2$(a), μB	Doubling Time, sec.	Δk_{eff}	$\frac{\Delta k_{eff}}{-\Delta B_z^2}$, cm^2
6	1	1.478 ±0.01	1.370 ±0.009	86.5 ±1.1	6.319	461.2
	2	1.549 ±0.01	1.435 ±0.009	82.5 ±1.3	6.526	454.7
	3	1.770 ±0.01	1.633 ±0.009	67.6 ±0.9	7.575	463.9
	4	1.829 ±0.01	1.688 ±0.009	64.4 ±1.0	7.853	465.2
	5	1.948 ±0.01	1.795 ±0.010	59.4 ±0.5	8.337	464.4
	6	2.101 ±0.01	1.936 ±0.010	53.5 ±0.5	8.980	463.8
7	7	1.128 ±0.01	1.314 ±0.020	89.0 ±0.9	6.182	470.4
	8	1.229 ±0.01	1.533 ±0.020	74.5 ±0.5	7.041	459.2
	9	1.262 ±0.01	1.573 ±0.021	72.2 ±0.5	7.209	458.2
	10	1.346 ±0.01	1.677 ±0.022	66.8 ±1.5	7.633	455.1
	11	1.407 ±0.01	1.751 ±0.022	62.3 ±0.6	8.049	459.7
	12	1.748 ±0.01	2.105 ±0.023	47.2 ±0.9	9.791	465.1

(a) $\mu B = 10^{-6}\ cm^{-2}$.

TABLE XIV

Sensitivity of $\Delta k_{eff}/-\Delta B_z^2$ to Changes in δ and T

Change in $\Delta k_{eff}/-\Delta B_z^2$ per 0.004 increase in δ = +1.6 cm^2.

Change in $\Delta k_{eff}/-\Delta B_z^2$ per 0.01 increase in T = +1.5 cm^2.

The vertical migration area was calculated using anisotropic two-group theory in the form:

$$(L_z^2 + \tau_z) = \frac{y - 2L_z^2\tau_z(B_r^2 + B_z^2) + yL_z^2\tau_z(B_r^2 + B_z^2)^2 - x}{1 - y(B_r^2 + B_z^2)} \quad (21)$$

where x is a correction for anisotropy given by

$$x = B_r^2\left[(L_z^2 - L_r^2)(y - \tau_z) + (\tau_z - \tau_r)(y - L_z^2)\right] \quad (22)$$

and

$$y = \Delta k_{eff}/-\Delta B_z^2$$

Because L_z^2, L_r^2, τ_z, and τ_r appear only in second order terms on the right hand side of equation (21), calculated values of these quantities are sufficiently accurate. All quantities used in this calculation are listed in Table XV. The anisotropy term, x, was taken as 1.16, the result of the anisotropy measurement discussed previously in this report.

The resulting values of $(L_z^2 + \tau_z)$ are given in Table XVI. The flags on the individual measurements represent a statistical combination of the experimental uncertainties only (ie, the uncertainties in measuring ΔH and doubling times), and do not include the systematic error due to the uncertainty in the calculated values of δ and T. The flag on the weighted mean at the bottom of the table includes the experimental uncertainties plus the systematic uncertainties.

The mean value of 492 ±11 cm^2 compares very favorably with the value of 483 ±14 cm^2 obtained by the copper poison method discussed in the previous section.

A calculation based on Benoist[8,9] using the input parameters given in Table VIII gives a value for M_z^2 of 527 cm^2, in relatively poor agreement with the measurements.

TABLE XV

Parameters Used in Obtaining $(L_z^2 + \tau_z)$ from Kinetics Experiments

	Loading No. 6	Loading No. 7
B_r^2, μB	203.9	173.7
B_z^2, μB	135.3	164.6
M_z^2/M_r^2	1.16	1.16
L_z^2, cm^2	286.4	286.4
τ_z, cm^2	240.7	240.7

TABLE XVI

Migration Area by Period Reactivity Measurements

Loading No.	Run	$(L_z^2 + \tau_z)$, cm^2
6	1	491.4 ±7.5
	2	482.7 ±6.7
	3	495.0 ±6.5
	4	496.7 ±6.8
	5	495.8 ±7.4
	6	491.7 ±7.6
7	7	504.5 ±7.6
	8	489.3 ±7.2
	9	486.3 ±7.2
	10	483.8 ±7.6
	11	489.9 ±7.6
	12	497.2 ±8.5
Mean value →		492 ±11

DIFFUSION COEFFICIENT MEASUREMENTS

Palmedo-Benoist Method

In the development of a general expression for the space dependent flux in a heterogeneous reactor, Palmedo and Benoist investigated the possibility of applying their results to the experimental determination of the radial diffusion coefficient[14]. Because their experimental results were quite encouraging, some similar measurements were performed in the EL-4 mockup.

The theory and development of the working expressions of the Palmedo-Benoist method are given in reference 14 and will not be described in detail here. In general, these authors show that the space dependent flux $\Phi(\vec{r})$ in a heterogeneous reactor can be represented by an expression that includes a macroscopic function $\Psi(\vec{r})$, a microscopic function $\phi(\vec{r})$, and an interaction term $\vec{\Phi}_1(\vec{r})$. This relation is written

$$\Phi(\vec{r}) = \Psi(\vec{r})\phi(\vec{r}) - \nabla\Psi(\vec{r}) \cdot \vec{\Phi}_1(\vec{r}) \qquad (23)$$

Further, an expression for $\vec{\Phi}_1(\vec{r})$ is developed which is shown to depend upon the radial diffusion coefficient.

To apply the theory to experiment, several expressions are developed that relate to (a) the measurement of the macroscopic flux distributions at different positions in a lattice cell, eg, to flux detector activations at the surface of the cladding of several fuel assemblies both towards and away from the center of the lattice, and (b) the measurement of the fine structure in one or more cells, eg, to foil activations at several angular positions around a fuel assembly.

For (a) above it is shown that for a one region cylindrical reactor

$$\Phi(\vec{r}) = \frac{\phi_c}{\phi_t} J_o (B_r r + \epsilon) \tag{24}$$

where

$$\epsilon \frac{\phi_c}{\phi_t} = B_r C_o \left(\frac{1}{c} - \frac{c}{b^2}\right) \tag{25}$$

c = distance from center of cell to the point of measurement, usually the edge of a rod or channel.

b = cylindricized radius of cell

ϕ_c = flux at radius c

ϕ_t = average flux in cell

B_r^2 = the radial buckling.

The term C_o is related to the radial diffusion coefficient D_r by

$$\frac{D_r}{D_m} = \frac{\phi_m}{\phi_t} + \frac{2\pi}{V_t} C_o \tag{26}$$

where

D_m = moderator diffusion coefficient

ϕ_m = average flux in the moderator

V_t = volume of the cell.

In equation (24), ϵ is positive or negative depending on whether the flux is measured on the side of the fuel assembly away from or toward the center of the lattice.

The development also shows that

$$\phi_1(\vec{r}) = C_o \left(\frac{1}{c} - \frac{c}{b^2}\right) \cos \alpha_o \tag{27}$$

where α_o is the angle made by a line drawn from the point of measurement to the cell center with a line drawn from the pile center to the cell center, ie, $\alpha_o = 180^o$ when the point of measurement is on the side of the assembly directed toward the center of the pile, and 0^o on the opposite side.

Two types of experiments using these developments were performed in the SE. Figures 12A and 12B show the experimental arrangement with gold pins placed at 45^o intervals on the outer surfaces of the fuel housing tubes. Data for the first type of experiment consisted of the (corrected) activations for the gold pins located directly toward and away from the center of the lattice. These data were fitted to equation (24) to determine both B_r and ϵ, which were substituted into equation (25) to determine C_o. Application of equation (26) then give experimental values of D_r/D_m.

The second type of experiment provided a more detailed test of the theory by comparing experimental values of Φ_1 with those predicted by equation (27). To obtain the experimental values, equation (23) was solved for $\Phi_1(\vec{r})$ setting $\Psi(\vec{r}) = J_o(B_r r)$

$$\Phi_1(\vec{r}) = \frac{\Phi(\vec{r})/J_o(B_r r) - \phi(\vec{r})}{(B_r)J_1(B_r r)/J_o(B_r r)} \qquad (28)$$

The pin activations around the fuel housings gave the values of $\Phi(\vec{r})$ at different radii r and angles α_o, while the activations of the pins on fuel assemblies at or near the pile center gave $\phi(\vec{r})$. Figures 19 and 20 show the resulting values of Φ_1 plotted against α_o for typical fuel assemblies. Comparison with the theoretical curves obtained from equation (27), also shown in Figures 19 and 20, shows that the experimental points have the approximate distribution required by the theory but fall below the theory in absolute magnitude. The two theoretical curves given in each figure represent the allowable spread in C_o determined from equation (25). The difference between the theory and the experiment is possibly due to the breakdown of the diffusion theory approximation of the interface between the void and moderator.

Experiments of the first type above were also performed in the PDP. Gold pins at $\alpha_o = 0^o$ and 180^o were placed on the housing tubes of selected fuel assemblies of the 156-assembly pile, as shown in Figure 21. Four such radial "traverses" were made at right angles to each other. The data were fitted to equation (24), where both B_r and ϵ were determined and then used to obtain C_o and D_r/D_m, as in the SE experiments.

The values of D_r/D_m obtained from the SE and PDP measurements are compared in Table XVII.

TABLE XVII

Summary of Palmedo-Benoist[14] D_r/D_m Measurements

	B_r^2, m^{-2}	D_r/D_m
SE, Moderator-centered	9.23 ±0.31	1.28 ±0.03
SE, Fuel-centered	8.87 ±0.12	1.29 ±0.02
PDP, Quadrant of pile		
1	1.81 ±0.02	1.38 ±0.05
2	1.79 ±0.01	1.25 ±0.01
3	1.80 ±0.01	1.27 ±0.03
4	1.81 ±0.01	1.27 ±0.01

The good agreement between the two facilities adds to the confidence in the method because the B_r^2 values are a factor of 5 apart. The calculated value of D_r/D_m using the Benoist method is 1.30.

The experimental method is straightforward and does not require the lattice to be perturbed other than by the placement of the flux detectors in the lattice. The values of B_r^2 obtained in fitting the gold pin activities to equation (24) are somewhat higher than those obtained from the interstitial traverses and the accuracy of the fit is somewhat poorer. The reason for this discrepancy is not clear.

Persson Substitution Method

A method of obtaining lattice bucklings by substitution techniques using a one group perturbation theory analysis was developed by Persson.[15] In this measurement it is necessary to obtain values of $\Delta D_z/D$ and $\Delta D_r/D$ resulting from the voiding of coolant channels in fuel assemblies. Methods given by Persson for measuring these parameters were used in this experiment in an attempt to obtain an independent verification of the effects of neutron streaming in the EL-4 mockup fuel assemblies.

The measurements were performed in the PDP in loading No. 7. A diagram of the lattice showing the locations of the test fuel assemblies is given in Figure 22. In the $\Delta D_z/D_z$ measurement, a single test fuel assembly was placed at the center of the lattice. This assembly was identical with the other fuel assemblies in the lattice, except that the bottom plug was removed from the housing tube to allow

D_2O to rise into the coolant channels. All other fuel assemblies and steel pipe assemblies in the lattice were air filled. The reactor was brought to critical, and the moderator height was measured. Helium pressure was then applied to the top of the test fuel assembly to partially expel the D_2O while the moderator height in the pile was adjusted to maintain criticality. The new critical moderator height and the helium pressure were then measured. The expulsion was performed in several steps, and the critical moderator height and helium pressure were measured at each step until the D_2O in the test fuel assembly was completely expelled. Finally, the pressure was reduced to zero, allowing the test fuel assembly to refill with D_2O. Then the critical moderator height was measured.

In the $\Delta D_r/D_z$ measurements, two test fuel assemblies were used at symmetrical positions 180° apart. Four critical runs were made, each one with the two test assemblies at a different radius. The four radial positions are designated A, B, C, and D in Figure 22. In each run the critical moderator height was measured, first with D_2O in the test housings, then with the D_2O completely expelled from the housings, and finally with the housings full of D_2O. In each run the three measurements were made by adjusting the moderator height to maintain criticality. The pile was then shut down, the test assemblies moved to a new radius, and the three measurements repeated.

The measured quantities for the two types of measurements are given in Table XVIII. In the $\Delta D_z/D$ measurement, the helium pressure was converted into terms of the fraction of fuel assembly which is gas filled. The change in critical moderator height, ΔH, is accurate to ±0.005 cm.

The results of the Persson analysis of these data are given in Table XIX. To facilitate comparison, the value of

$$\frac{D_z^{air} - D_z^{D_2O}}{D_z^{air}}$$

that results directly from the measurement is also given in terms of

$$\frac{D_z^{air} - D_z^{D_2O}}{D_z^{D_2O}}$$

The value 0.512 measured in the present experiments agrees favorably with an earlier value of 0.529 measured[10] for the same fuel assemblies at a slightly different lattice pitch (23.7 cm triangular).

The results of the $\frac{D_r^{air} - D_r^{D_2O}}{D_z^{air}}$ measurements are also given in Table XIX. This measurement had also been performed previously with this type of fuel assembly, but in a reference lattice of D_2O-filled assemblies; in this experiment the reference lattice was air filled. The results do not agree with the earlier experiments or with calculations. Although the reasons for the discrepancy have not been examined in detail, a systematic error involving the combination of the large bottom reflector and the voided reference lattice is probably responsible. Because of this anomoly it is impossible to obtain a satisfactory measure of the anisotropy in this lattice from these results.

TABLE XVIII

Measured Data, Persson $\Delta D/D$ Measurements

$\Delta D_z/D_z$	Step No.	ΔH[a], cm	$-\Delta B_z^2$, μB	Fraction of Test Assembly Gas Filled
	1	0	0	0
	2	0.368	0.463	0.324
	3	0.373	0.472	0.415
	4	0.373	0.473	0.450
	5	0.368	0.466	0.499
	6	0.371	0.472	0.544
	7	0.371	0.473	0.566
	8	0.371	0.474	0.603
	9	0.378	0.483	0.675
	10	0.409	0.521	0.741
	11	0.612	0.779	0.934
	12	0.356	0.459	0.571
	13	0.358	0.462	0.434
	14	0	0	0

$\Delta D_r/D_z$	Test Assembly[b] Position	Radius in Pile, cm	Change in Critical Conditions Upon Expelling D_2O from Test Assemblies: ΔH, cm	$-\Delta B_z^2$, μB
	A	48.95	1.16	-1.477
	B	87.97	0.96	-1.214
	C	114.29	0.74	-0.936
	D	131.60	0.69	-0.877

(a) Change in critical moderator height from Step No. 1. D_2O height increased upon expelling D_2O from assembly.
(b) See Figure 22.

TABLE XIX

Results of Persson ΔD/D Measurements in PDP

$$\frac{D_z^{air} - D_z^{D_2O}}{D_z^{air}} = 0.339$$

$$\frac{D_z^{air} - D_z^{D_2O}}{D_z^{D_2O}} = 0.512$$

$$\frac{D_r^{air} - D_r^{D_2O}}{D_z^{air}} = 0.280$$

$$\frac{D_r^{air} - D_r^{D_2O}}{D_z^{D_2O}} = 0.423$$

GAP CORRECTION CALCULATION

The vertical buckling measurements for some of the PDP loadings must be corrected for the buckling change caused by the gap where two fuel sections were joined. Figure 13 shows the location of the gap in the fuel assembly; Figure 14 shows the water heights for the different lattice loadings in relation to the gap. The gap causes a change in f, the thermal utilization; in L^2, the thermal diffusion area; and in p, the resonance escape probability. The flux peaking causing the f and L^2 changes can be measured by foil activations in the fuel assembly. Resonance escape probability changes can be estimated by calculations.

To determine the gap correction, the buckling change was calculated for a section of fuel assembly of arbitrary length (but longer than 3 mean free paths for lattice neutrons) in a flat vertical flux. Then the vertical buckling correction for a lattice containing the gap was determined by flux-squared weighting of the flat flux ΔB_z^2 in the measured vertical buckling of the lattice.

The measurement of the flux peaking at the gap was made by placing copper foils between fuel pellets of the four different types of rods in a representative assembly. Foil activities were corrected to a flat vertical flux as shown in Figure 23.

Consider an 18 cm section of fuel assembly that includes the gap. If the gap were not present, f would be that of an infinite lattice. When the gap is present in a flat flux, f changes to f'.

$$\frac{1}{f} = \frac{X_f + X_m + X_{Al}}{X_f} \quad \text{where } X_i = (\phi \Sigma_a V)_i \tag{29}$$

$$\frac{1}{f'} = \frac{X'_f + X_m + X_{Al} + X'_{Al}}{X'_f} \tag{30}$$

$$\frac{1}{f'} = \left(\frac{1}{f}\right) \frac{\phi}{\phi'_a} + 1 - \frac{\phi}{\phi'_a} + \frac{\phi''}{\phi} \cdot \frac{\Sigma_a^{Al}}{\Sigma_a^f} \cdot \frac{1-a}{a} \tag{31}$$

f (from calculation) = 0.9449

a = fraction of fuel section that is fuel = 0.9333

ϕ = thermal neutron flux in fuel assembly without gap

ϕ' = thermal neutron flux in fuel assembly with gap

ϕ'' = thermal neutron flux in aluminum connectors between fuel rods

$\frac{\phi}{\phi'} = 0.9899$; $\frac{\phi''}{\phi} = 1.137$

$\Sigma_a(Al) = 0.0123\ cm^{-1}$; $\Sigma_a(fuel) = 0.169\ cm^{-1}$

$f' = 0.9362$ (flat flux)

$\frac{\Delta f}{f} = \frac{f - f'}{f} = 9.2 \times 10^{-3}$.

Two effects are included in $\Delta p/p$ in going from a fuel section without a gap to a section with a gap. First, the fuel-to-moderator ratio is reduced because fuel is removed from the section. Second, the resonance integral, RI, changes because of a reduction of the mass of UO_2 and an increase in the effective surface.

$$1 - p = \frac{N_f}{\xi \Sigma_s} \frac{V_U}{V_m} RI \qquad (32)$$

$$\frac{\Delta p}{p} = \frac{1-p}{p} \left[\left(\frac{V_U}{V_m} \right)^{-1} \Delta \frac{V_U}{V_m} + \frac{\Delta RI}{RI} \right] \qquad (33)$$

$$\left(\frac{V_U}{V_m} \right)^{-1} \Delta \frac{V_U}{V_m} \cong (1 - a) = 0.0667$$

$$\frac{\Delta RI}{RI} = \frac{13.3}{RI} \left(\frac{S}{M} \right)^{\frac{1}{2}} \left[\frac{\Delta S}{M} - \frac{S}{M} \frac{\Delta M}{M} \right] = -2.97 \times 10^{-2}$$

$$\frac{\Delta p}{p} = -3.6 \times 10^{-3} \text{ (flat flux).}$$

The correction to be applied to the measured bucklings because of the fuel gap is determined by calculating the difference in buckling between the fuel section with the gap and that of a fuel rod with no gap.

Starting from a two group formulation, the buckling difference in the gap is given by

$$k_\infty = \eta \epsilon p f = (1 + L^2 B^2)(1 + \tau B^2) \qquad (34)$$

$$\Delta k_\infty / k = \frac{\Delta f}{f} + \frac{\Delta p}{p} = \frac{(L^2 + \tau)\, \Delta B^2 + B^2 \Delta L^2}{(1 + L^2 B^2)(1 + \tau B^2)} \qquad (35)$$

$$\Delta B^2 = \left[\frac{\Delta f}{f} + \frac{\Delta p}{p} \right] (1 + L^2 B^2)(1 + \tau B^2) - \frac{\Delta f}{f} L^2 B^2 \qquad (36)$$

where $\Delta L^2 = \frac{\Delta f}{f} L^2$

$$\Delta B^2 = 0.11 \text{ m}^{-2} \text{ (flat flux).}$$

Figure 24 shows the net buckling correction as a function of vertical buckling. These results were applied wherever necessary.

ANCILLARY MEASUREMENTS

Moderator Flux Traverse

To determine if the placement of the copper poison tubes at the corners of the lattice cells appreciably suppressed the moderator flux, an experimental flux traverse was made, using copper wire, along the diagonal of a square lattice cell that contained a copper tube and, for reference, a cell that did not have copper. The results of the traverses are shown in Figure 25, normalized to THERMOS[11] calculations for the fuel cell and copper tube. The traverse through the copper-containing cell shows some suppression when compared to the D_2O traverse, but for most of the points it is not a significant amount because of overlapping error bars. On the basis of this experiment, the change in the moderator disadvantage factor was considered negligible for the determination of $(L_z^2 + \tau_z)$.

Reflector Savings

The critical buckling was determined for four lattice loadings that had D_2O reflectors. In two of the loadings - the 332 and 120 assembly piles - both the vertical and radial buckling components were measured by pin irradiations. For the other two pile sizes, only the vertical buckling was determined by critical water height means. The radial buckling was then inferred from one of the other pile sizes and the anisotropy in migration area as described previously (see page 15). Reflector saving is defined as the difference between the extrapolated and cylindricized radii of the core. Reflector thickness is defined as the difference between the radius of the reactor tank and the cylindricized radius of the core.

Figure 26 shows reflector savings as a function of reflector thickness for all reflected lattices, including the two points from the SE.

ACKNOWLEDGEMENT

The authors wish to express their appreciation to P. A. Lourme, Centre D'Études Nucléaires de Saclay, France, for his many helpful suggestions and stimulating technical discussions during his visit to this laboratory in the early phases of this work.

REFERENCES

1. Horowitz, J. "Le Projet El 4". Energie Nucléaire 3, No. 6, pp. 369-71 (1961).

2. Bailley Du Bois, B. and R. Naudet. "Presentation de l'avant-Projet EL 4". Energie Nucléaire 3, No. 6, pp. 372-89 (1961).

3. Dunklee, A. E. The Heavy Water System of the Process Development. E. I. du Pont de Nemours & Co., Savannah River Laboratory, Aiken, S. C. USAEC Report DP-567 (1961).

4. Towler, O. A., Jr. and J. W. Wade. "Exponential Measurements in Heavy-Water Systems". Chem. Eng. Progr. Symp. Ser. 52, No. 19, 177-81 (1956).

5. Axtmann, R. C., et al. Initial Operation of the Standard Pile. E. I. du Pont de Nemours & Co., Savannah River Laboratory, Aiken, S. C. USAEC Report DP-32 (1953).

6. Graves, W. E. R-3/Adam Lattice Buckling Measurements in the Process Development Pile. E. I. du Pont de Nemours & Co., Savannah River Laboratory, Aiken, S. C. USAEC Report DP-598 (1961).

7. Driggers, F. E. "BSQ - An IBM-704 Code to Calculate Heavy Water Lattice Parameters". Panel on Heavy Water Lattices, International Atomic Energy Agency, Vienna, Austria, February 18-22, 1963.

8. Benoist, P. General Formulation of the Diffusion Coefficient in a Heterogeneous Medium Allowing Cavities. Commissariat a l'Energie Atomique, Paris, France. Report SPM-522 (1958).

9. Benoist, P. A Simple New Expression for the Radical Diffusion Coefficient for Fueled Channels. Commissariat a l'Energie Atomique, Centre d'Etudes Nucléaires, Saclay, France. Report SPM-710 (1962).

10. Graves, W. E. Analysis of the Substitution Technique for the Determination of D_2O Lattice Bucklings. E. I. du Pont de Nemours & Co., Savannah River Laboratory, Aiken, S. C. USAEC Report DP-832 (1963).

11. Honeck, H. C. THERMOS. A Thermalization Transport Theory Code for Reactor Lattice Calculations. Brookhaven National Laboratory, Upton, N. Y. USAEC Report BNL-5826 (1961).

12. Baumann, N. P. Resonance Integrals and Self-Shielding Factors for Detector Foils. E. I. du Pont de Nemours & Co., Savannah River Laboratory, Aiken, S. C. USAEC Report DP-817 (1963).

13. Keepin, G. R. "Neutron Data for Reactor Kinetics". Nucleonics 20, No. 8, pp. 150-56 (1962).

14. Palmedo, P. E. and P. Benoist. "Interaction of Macroscopic Flux and Fine Structure in Heterogeneous Reactors." IAEA Symposium on Exponential and Critical Experiments, Amsterdam (September 1963).

15. Persson, R. One Group Perturbation Theory Applied to Substitution Measurements with Void. RFX-74 (1961).

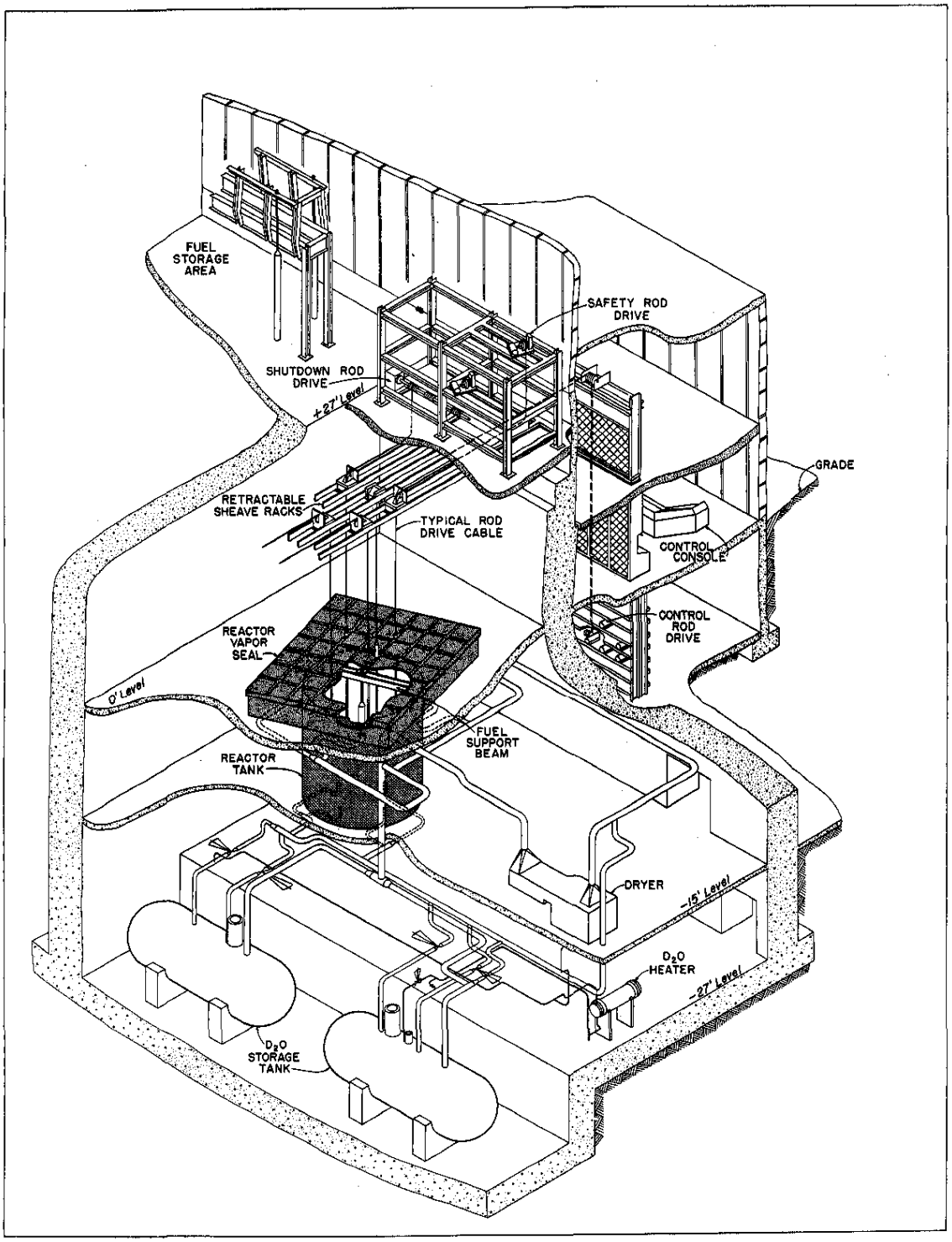

FIG. 1 ISOMETRIC DRAWING OF PROCESS DEVELOPMENT PILE

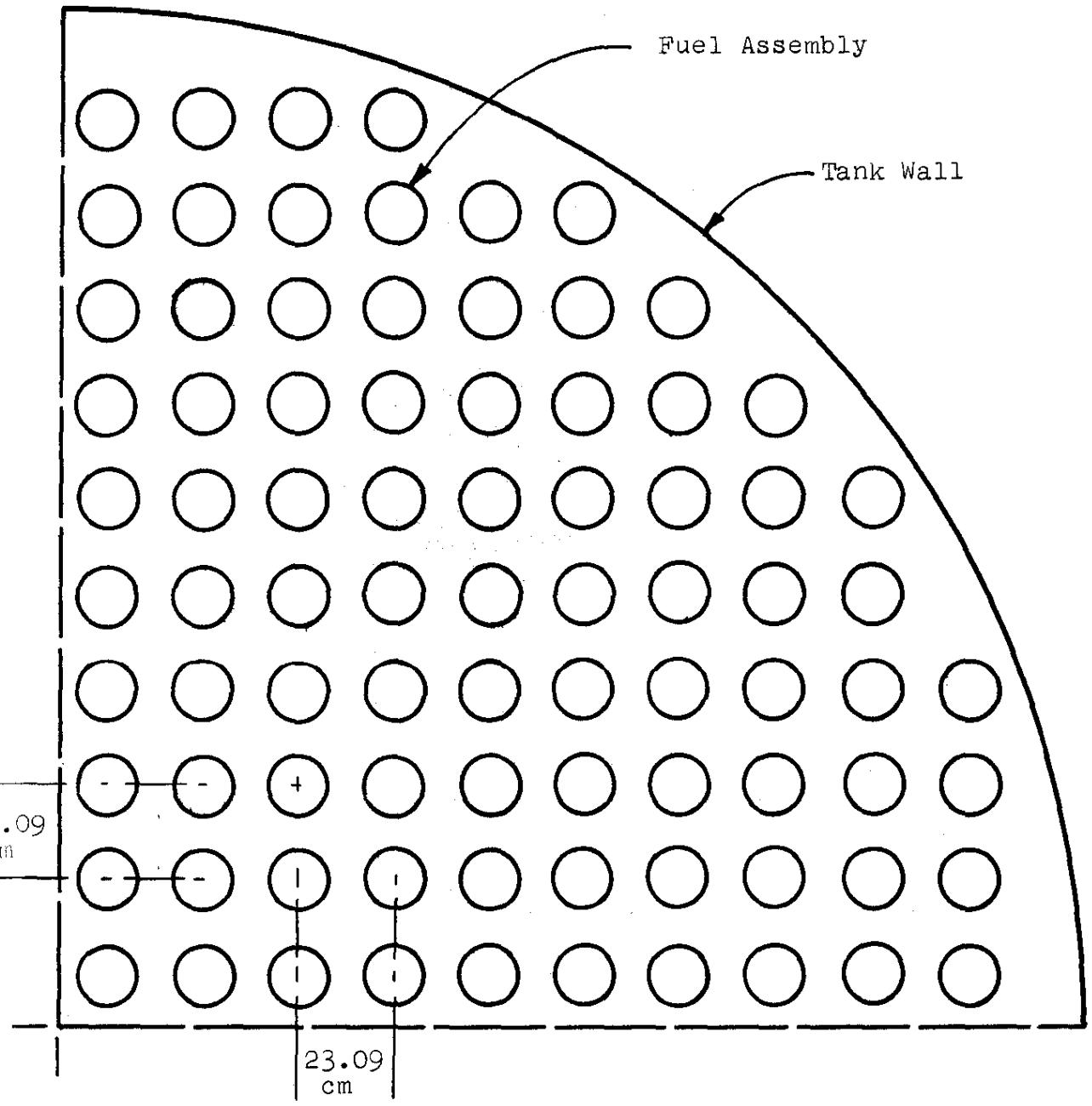

FIG. 2 QUADRANT OF PDP LOADING NO. 1
332 Fuel Assemblies

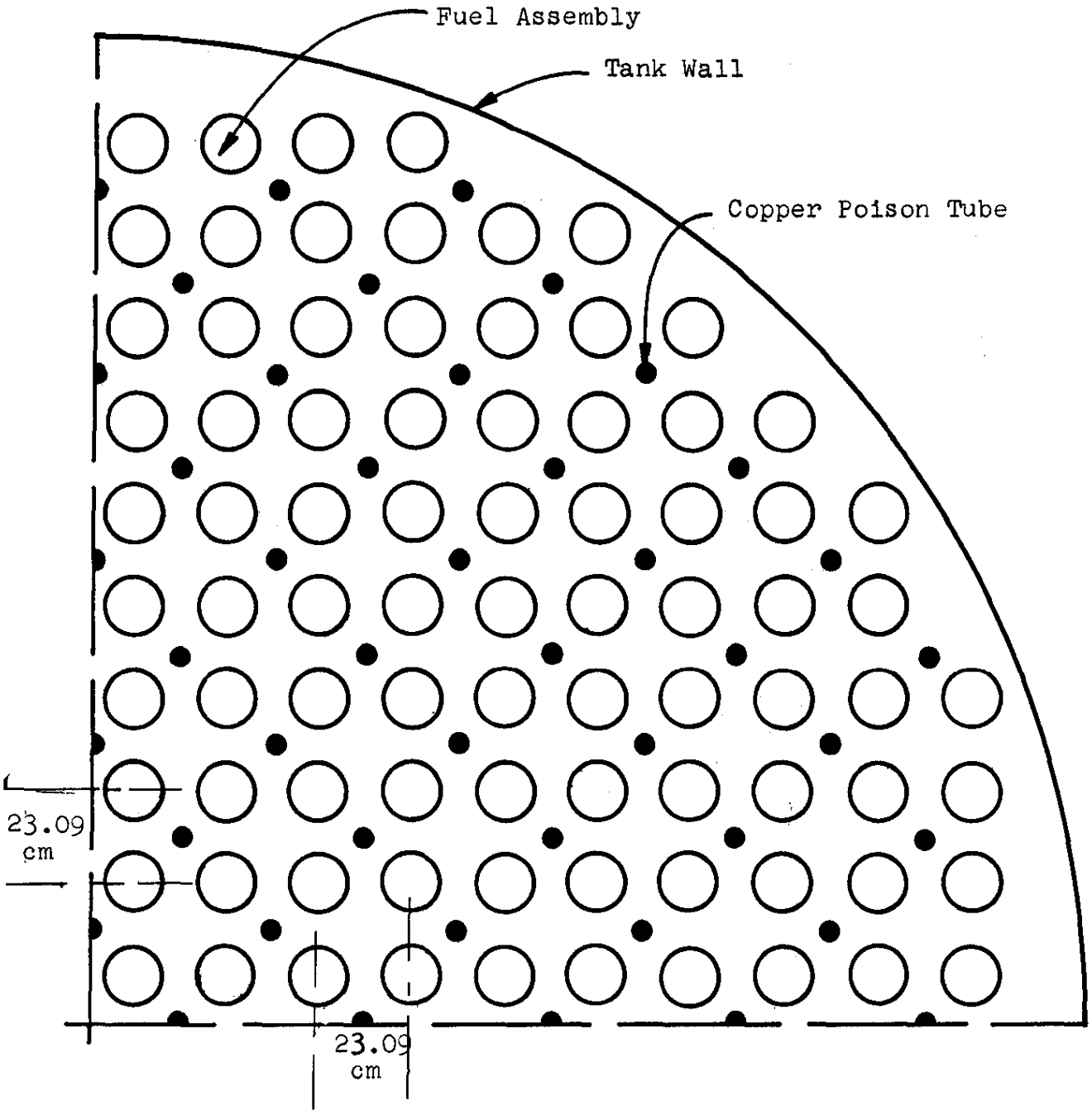

FIG. 3 QUADRANT OF PDP LOADING NO. 2
332 Fuel Assemblies
156 Copper Tubes

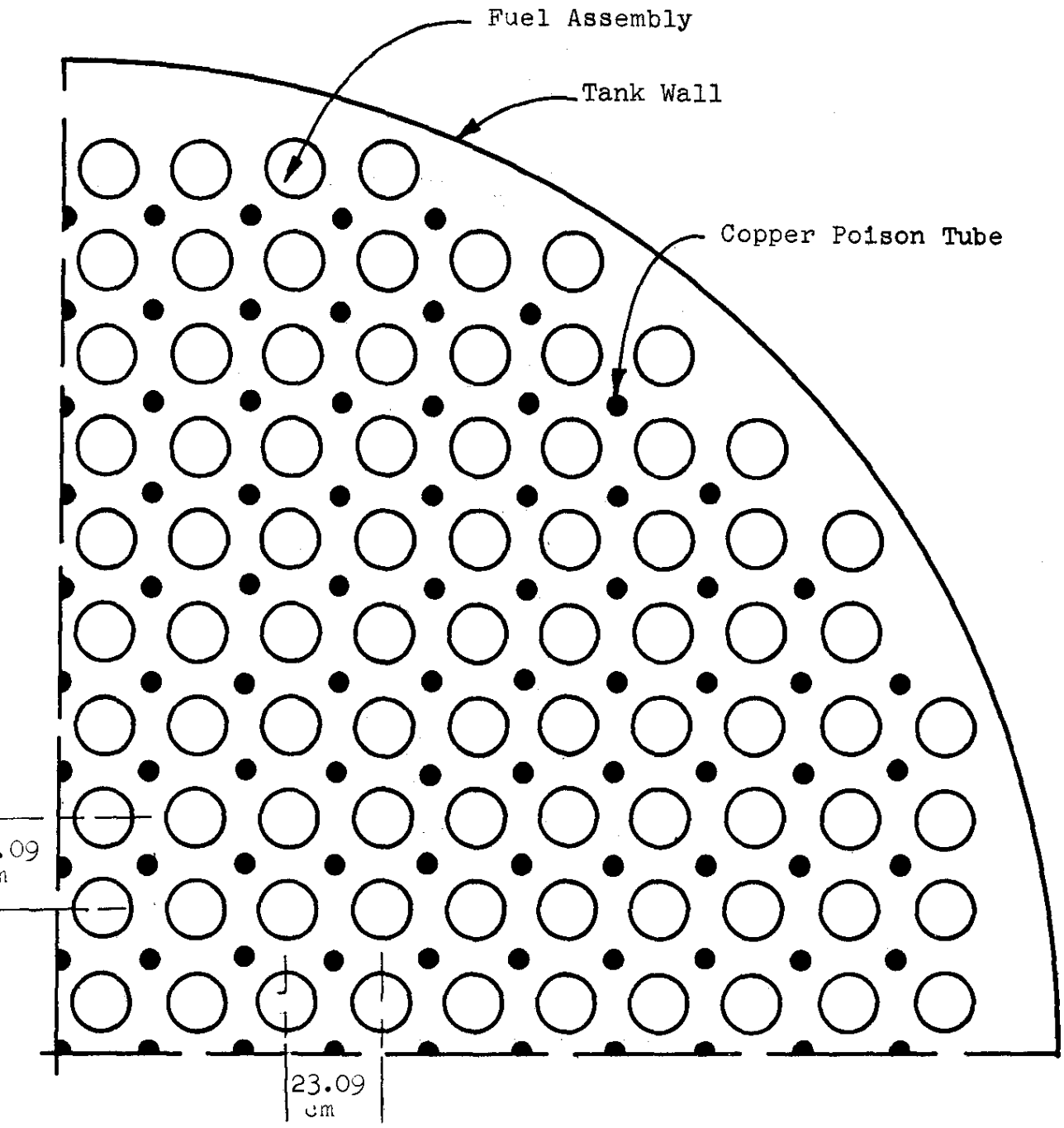

FIG. 4 QUADRANT OF PDP LOADING NO. 3

332 Fuel Assemblies
301 Copper Tubes

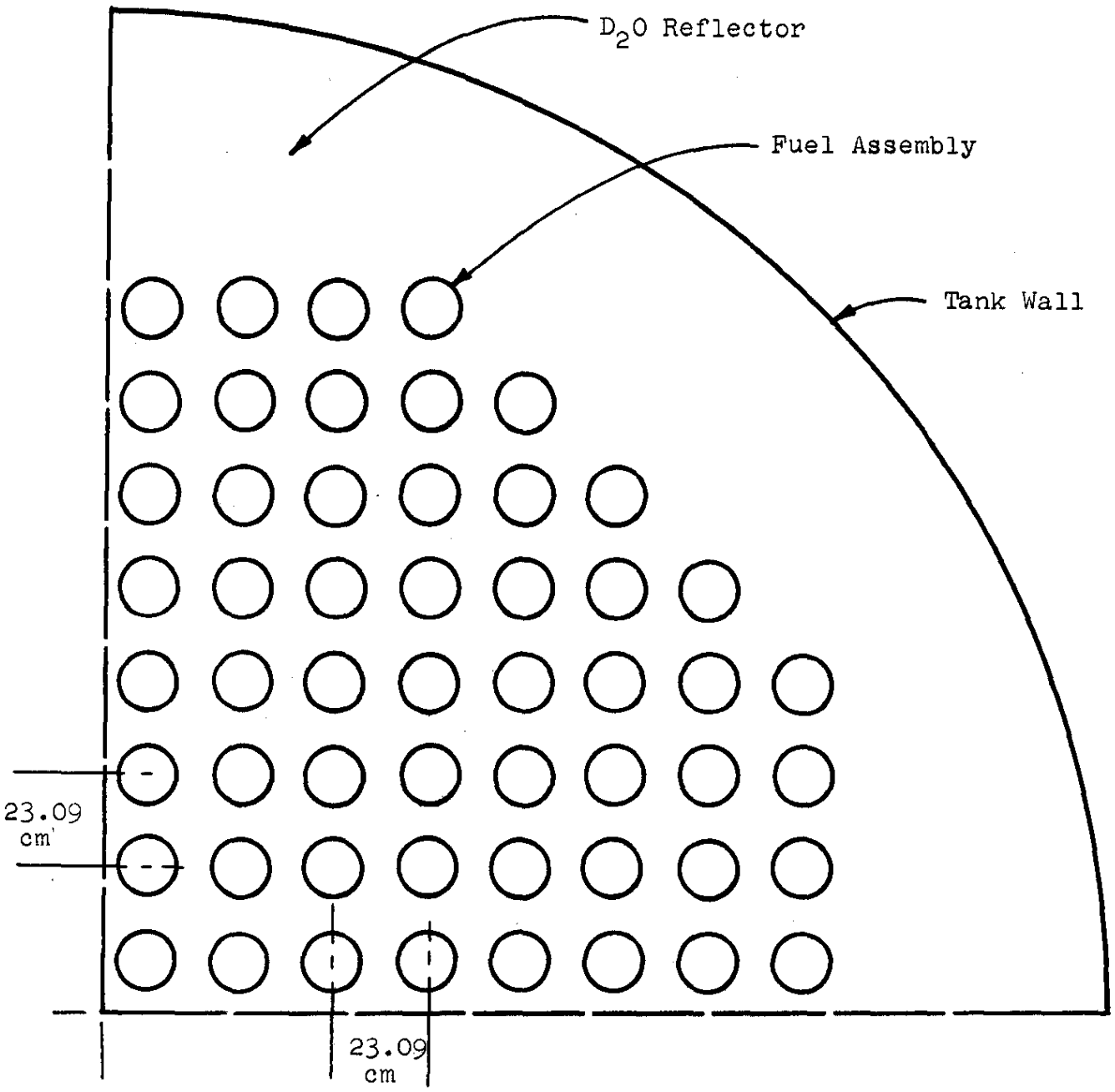

FIG. 5 QUADRANT OF PDP LOADING NO. 4
216 Fuel Assemblies
D_2O Reflector

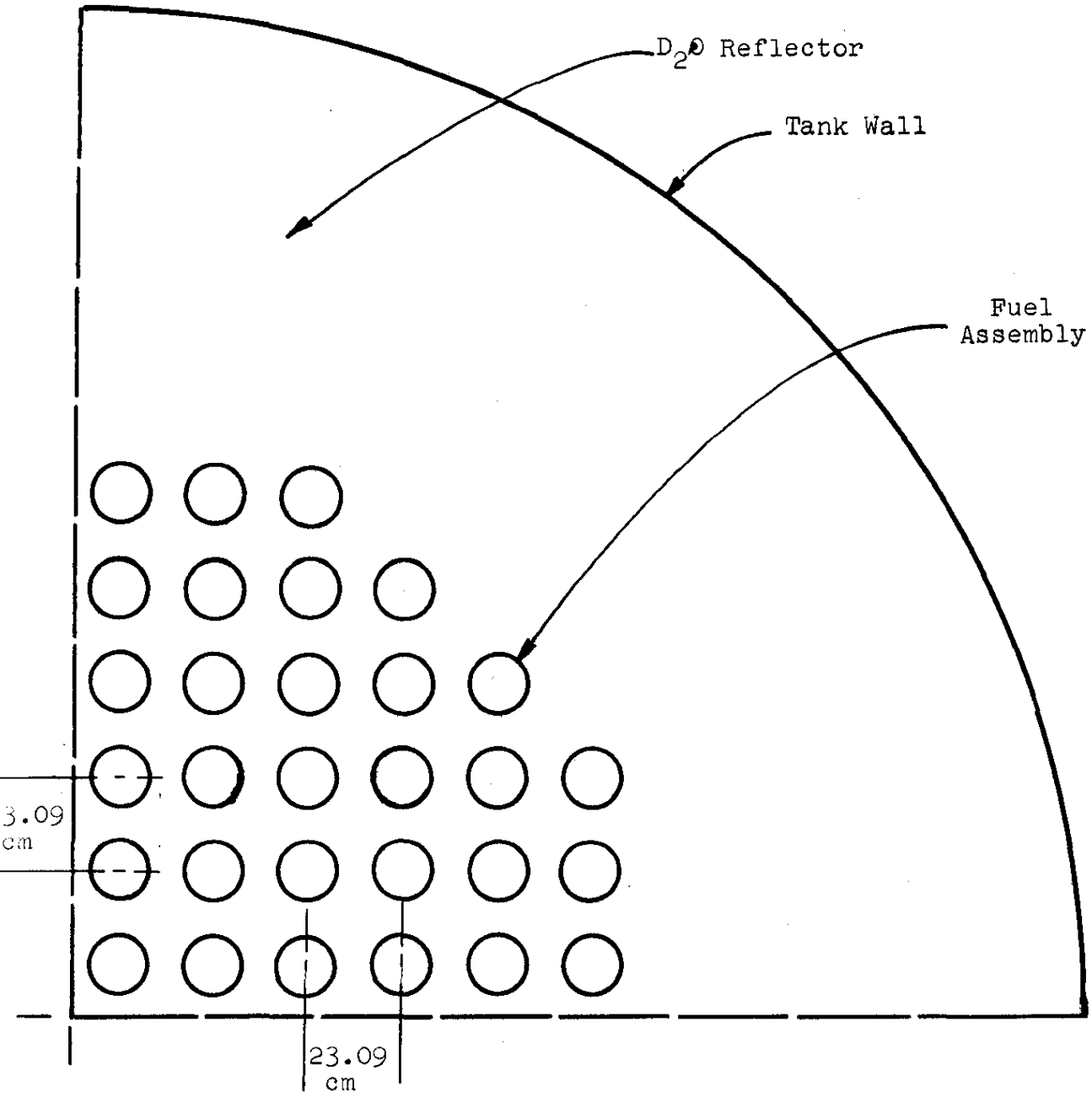

FIG. 6 QUADRANT OF PDP LOADING NO. 5

120 Fuel Assemblies

D_2O Reflector

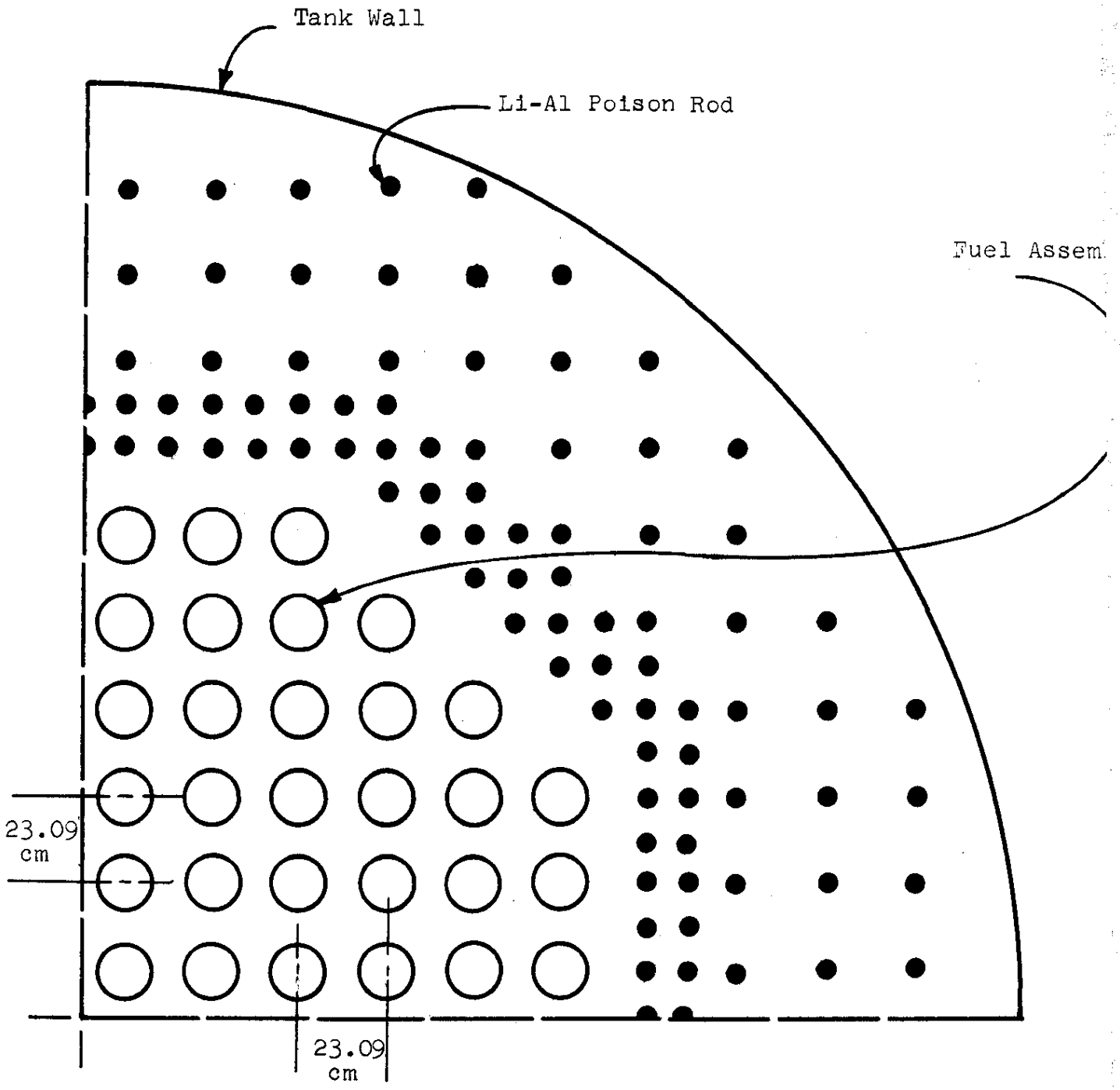

FIG. 7 QUADRANT OF PDP LOADING NO. 6
120 Fuel Assemblies
Li-Al Poisoned Reflector

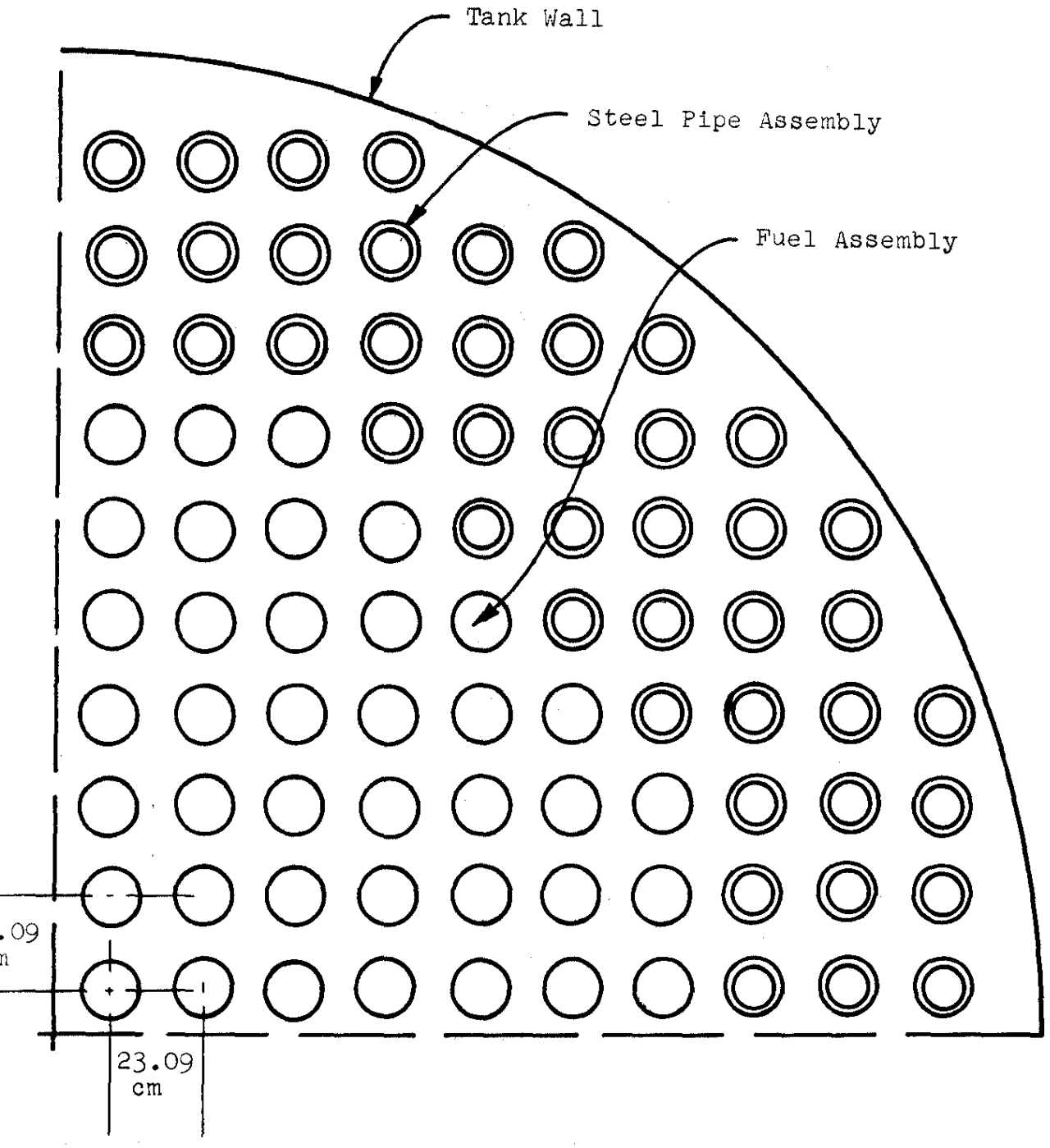

FIG. 8 QUADRANT OF PDP LOADING NO. 7
156 Fuel Assemblies
160 Steel Pipe Assemblies

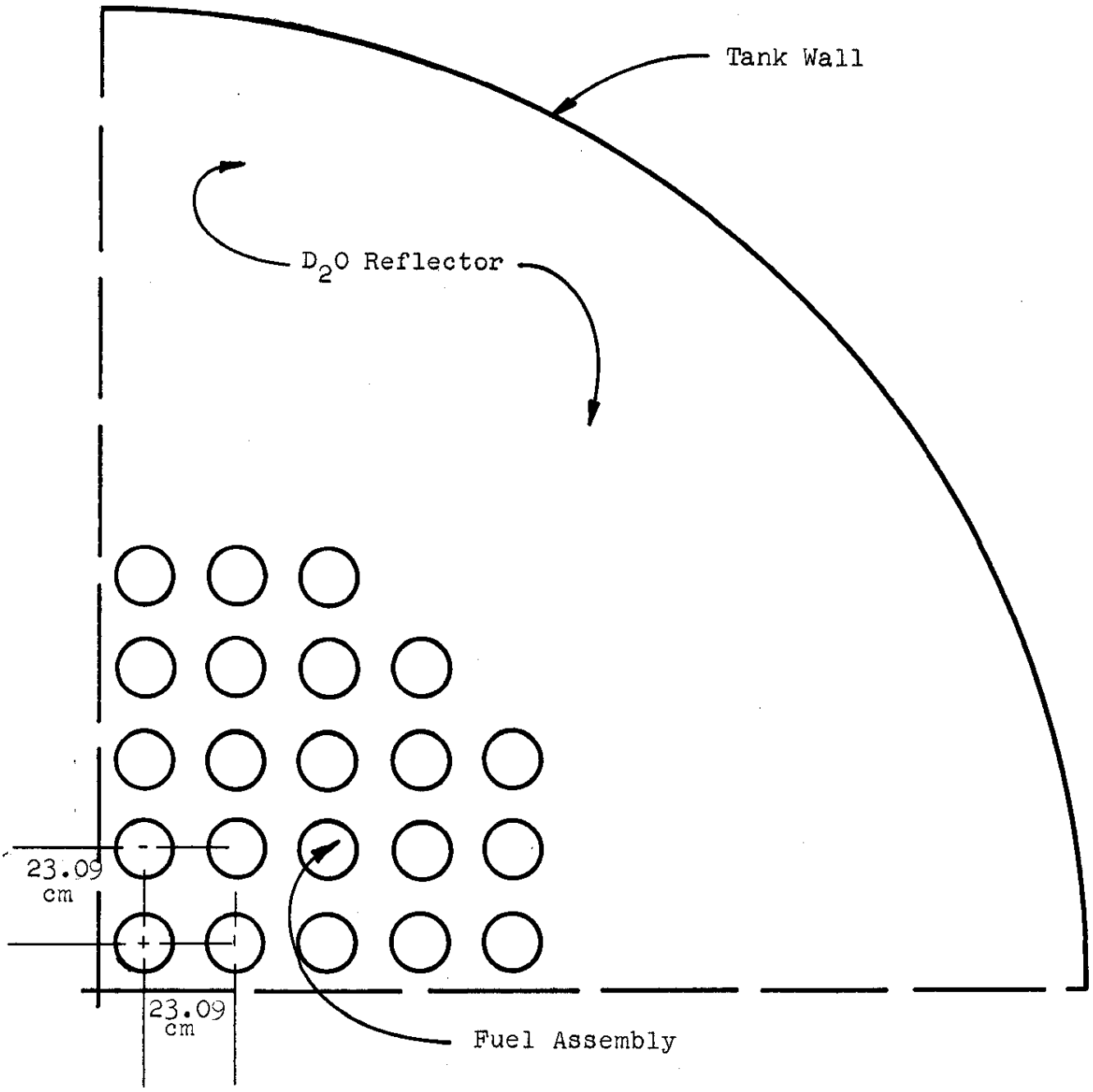

FIG. 9 QUADRANT OF PDP LOADING NO. 8
88 Fuel Assemblies
D_2O Reflector

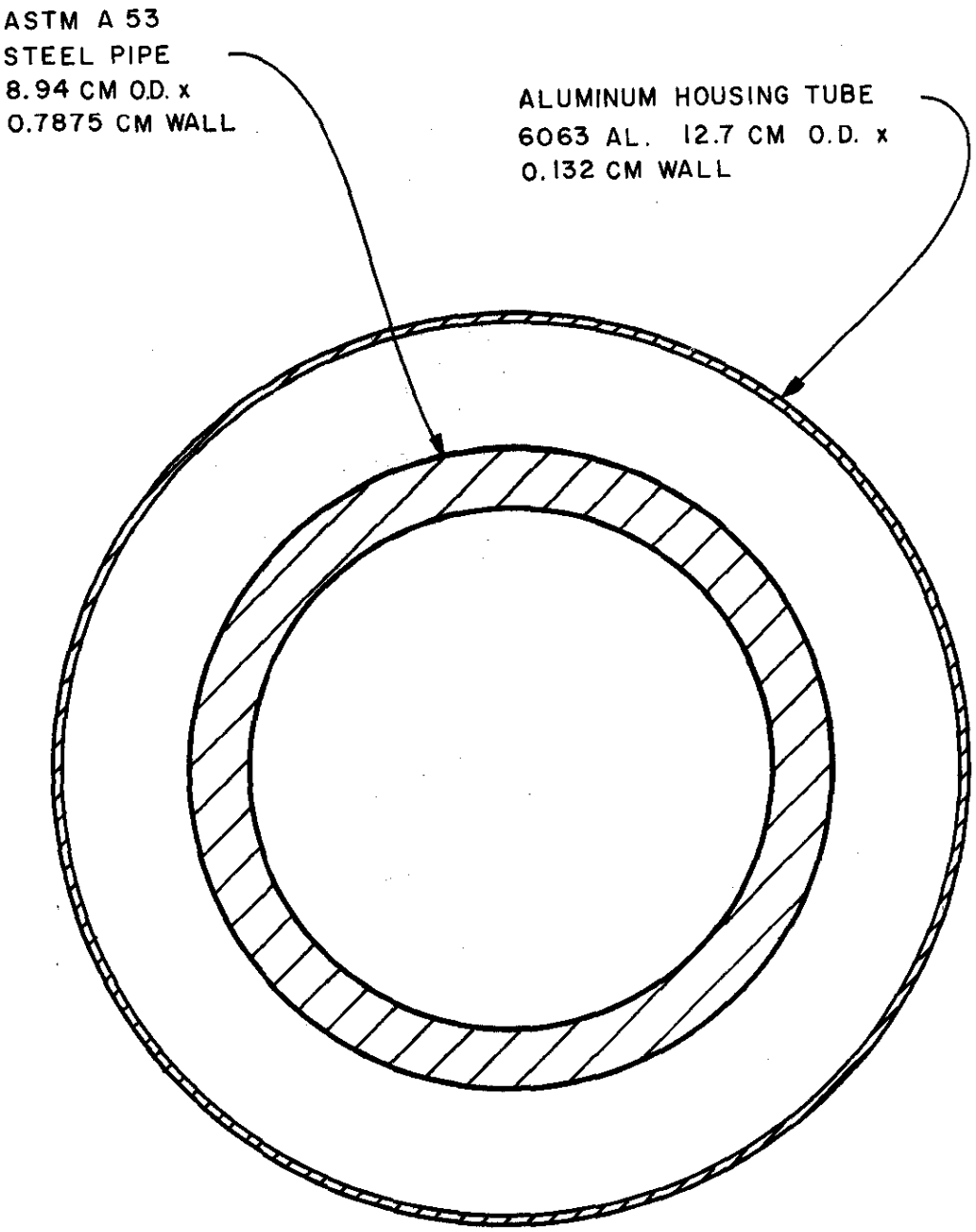

FIG. 10 CROSS SECTION OF STEEL PIPE ABSORBER ASSEMBLY

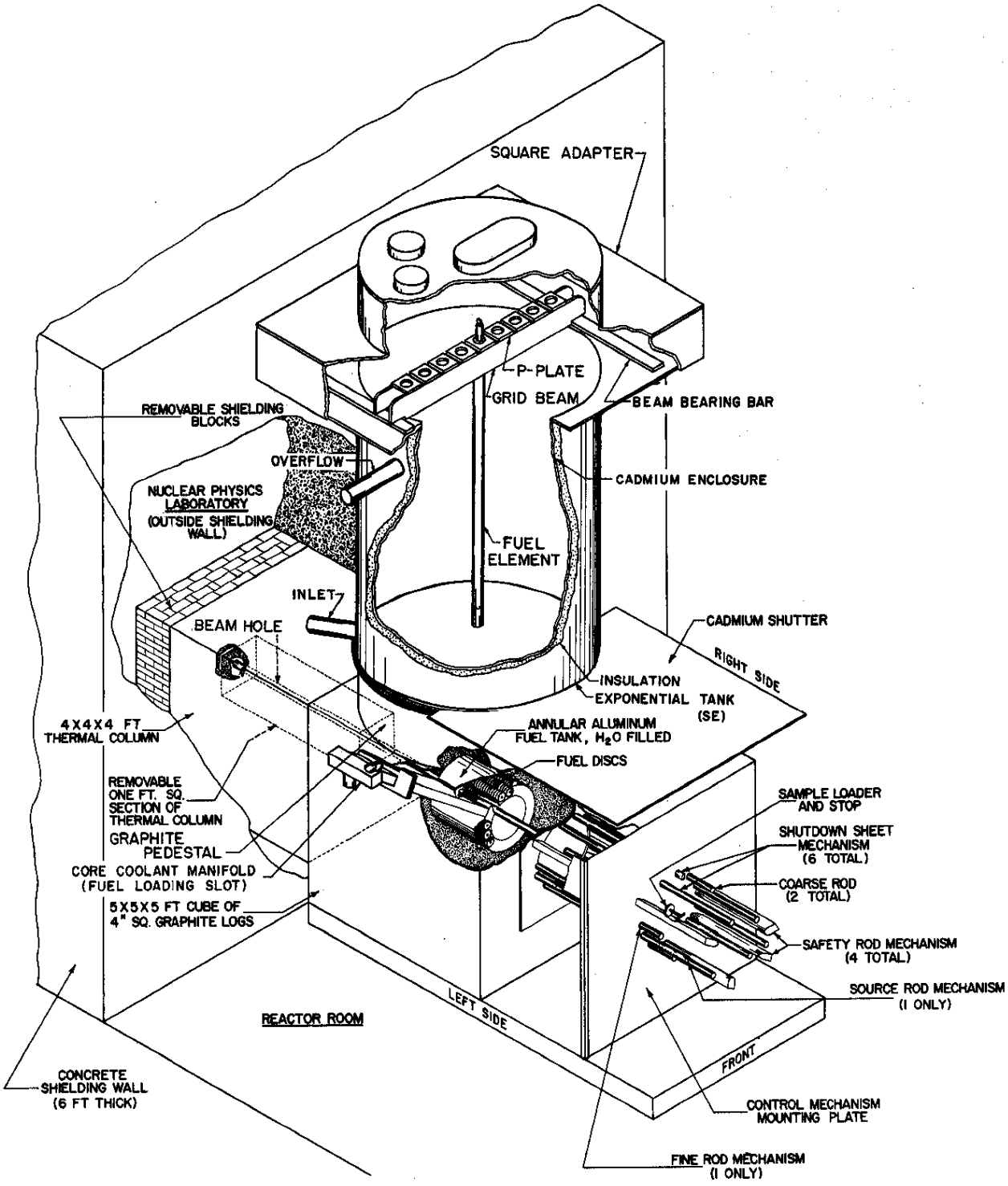

FIG. 11 ISOMETRIC VIEW OF STANDARD PILE AND EXPONENTIAL TANK

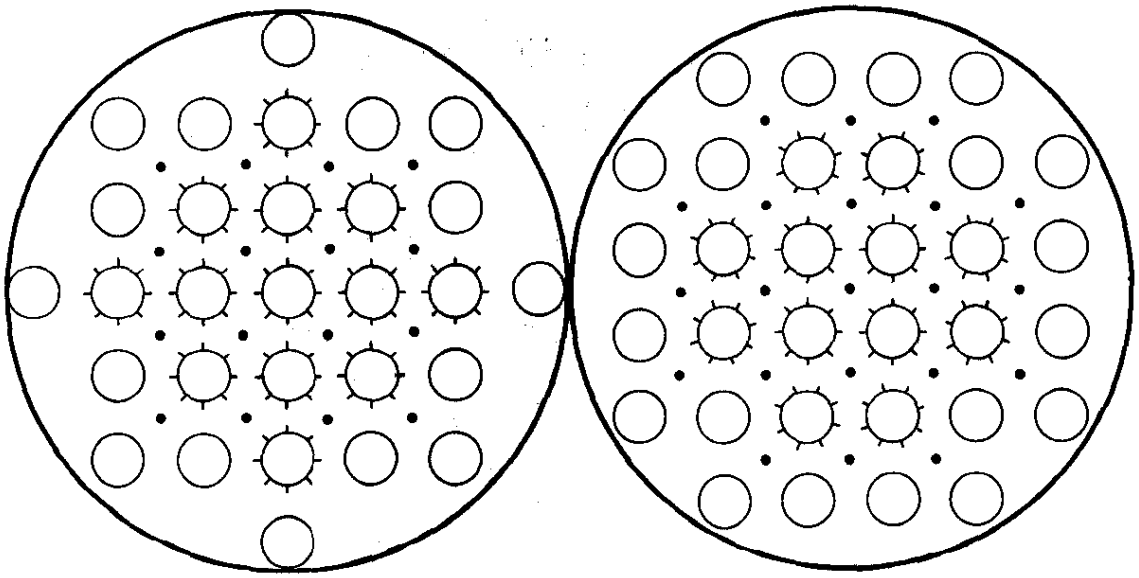

A

FUEL
CENTERED

B

MODERATOR
CENTERED

•-- POSITION OF COPPER POISON TUBES AND GOLD PIN POSITIONS FOR RADIAL BUCKLING MEASUREMENTS

POSITION OF GOLD PINS FOR PALMEDO-BENOIST MEASUREMENT

FIG. 12 SE LOADINGS

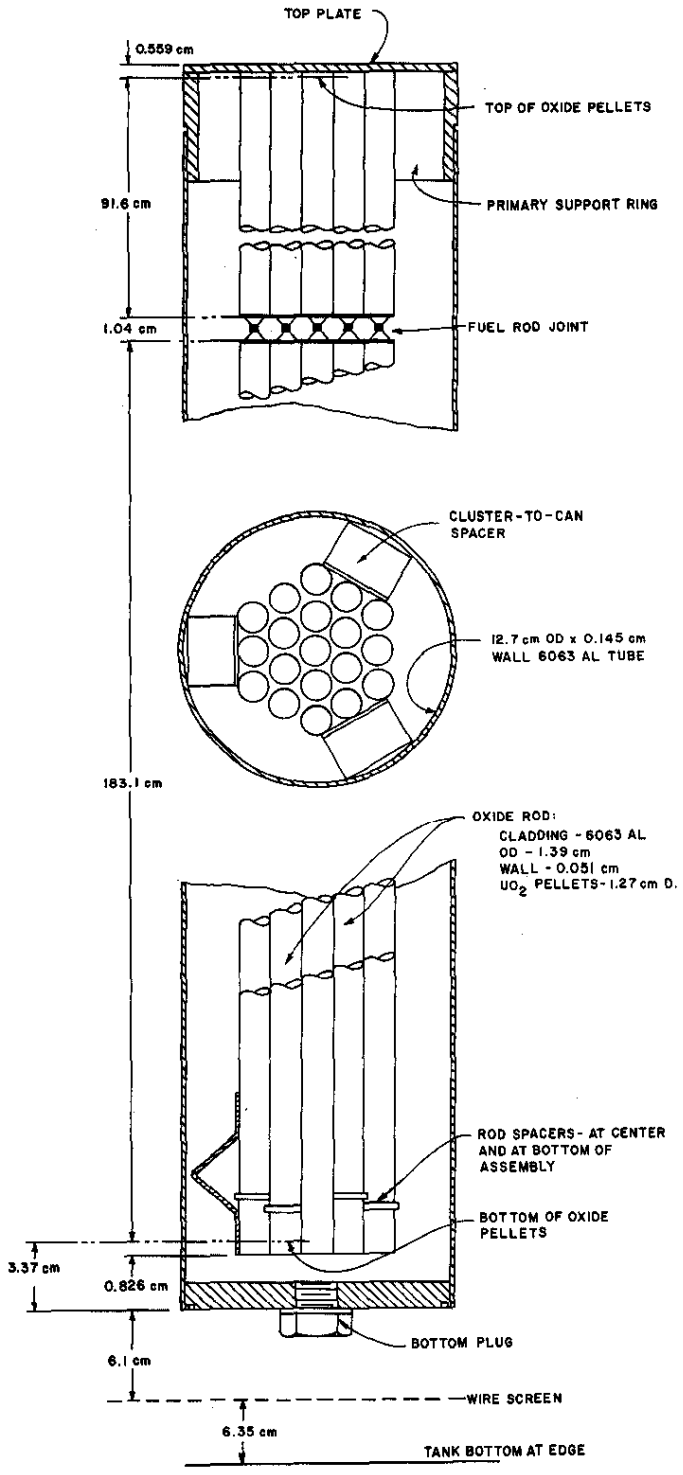

FIG. 13 NINETEEN-ROD UO_2 FUEL ASSEMBLY

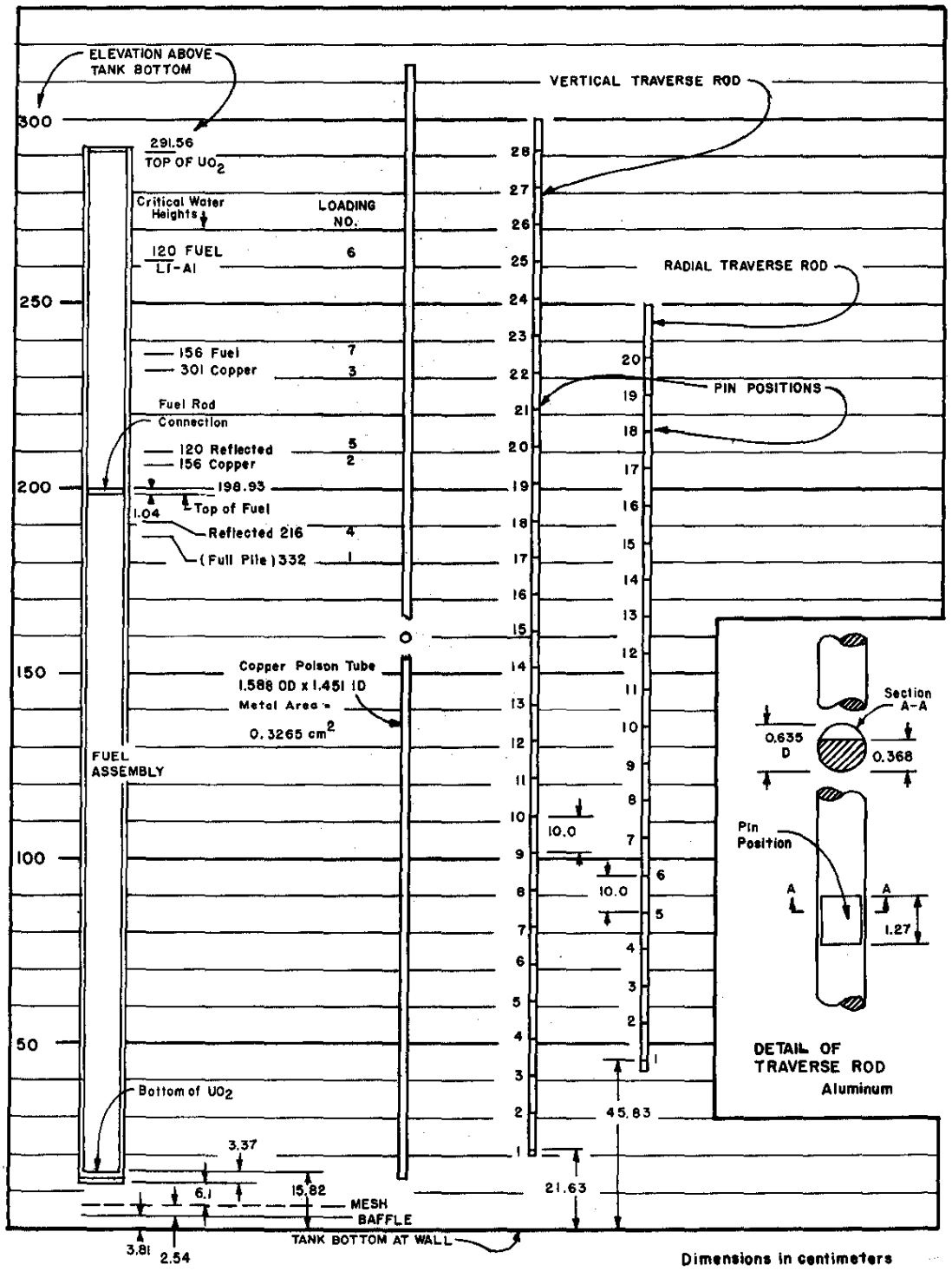

FIG. 14 VERTICAL SECTION OF LATTICE COMPONENTS IN EL-4 EXPERIMENTS

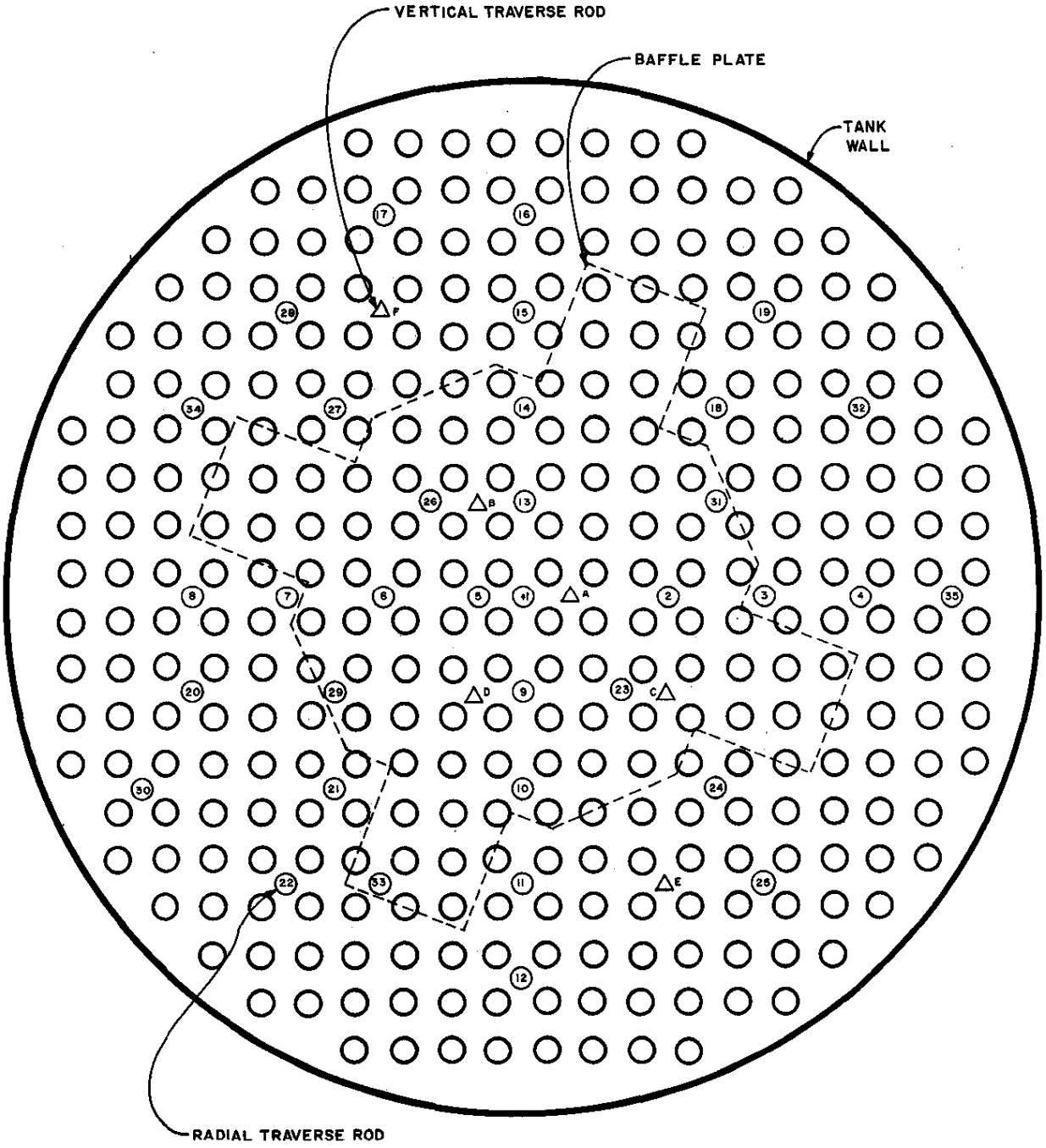

FIG. 15 GOLD PIN LAYOUT LOADING NO. 1

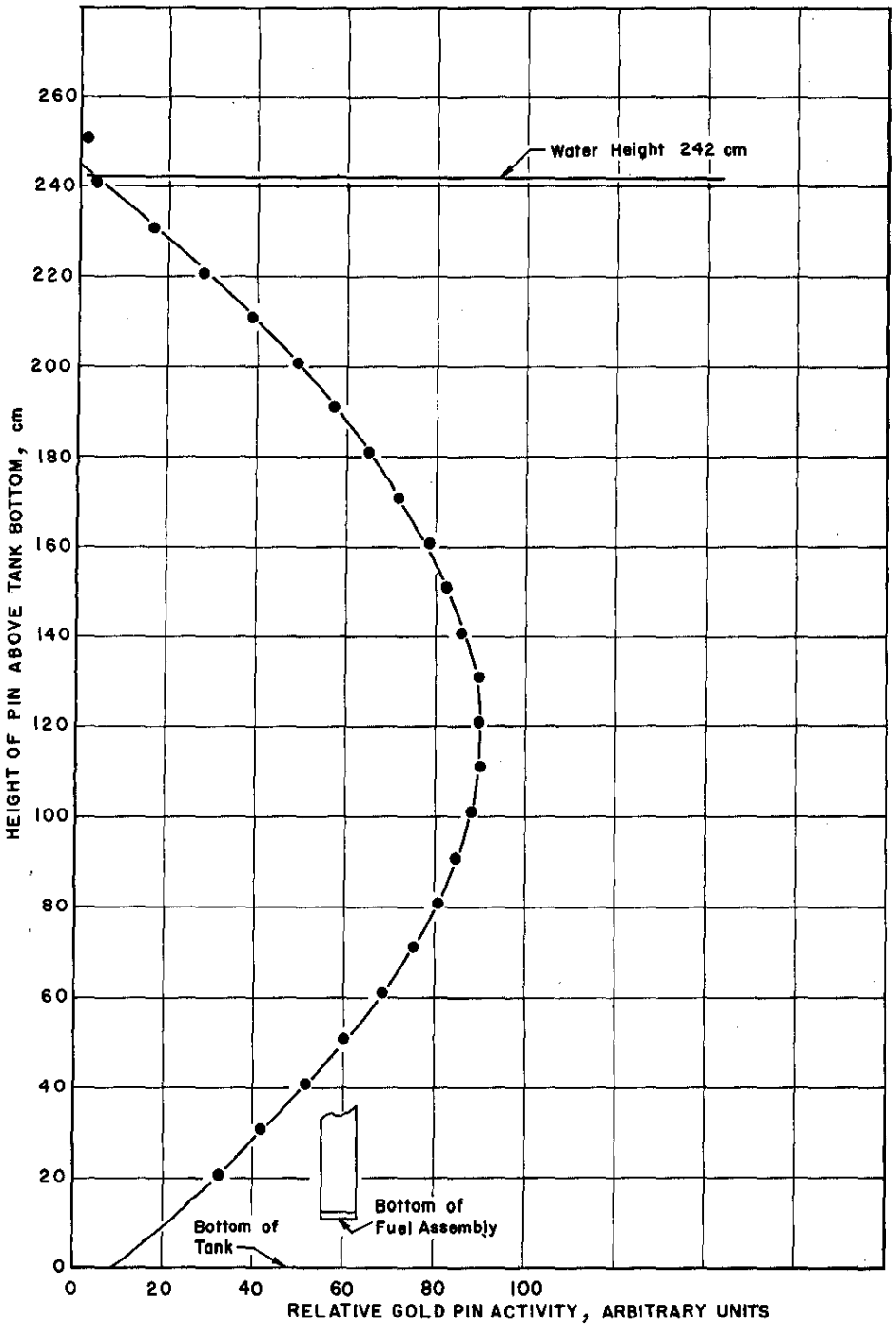

FIG. 16 VERTICAL GOLD PIN TRAVERSE LOADING NO. 7

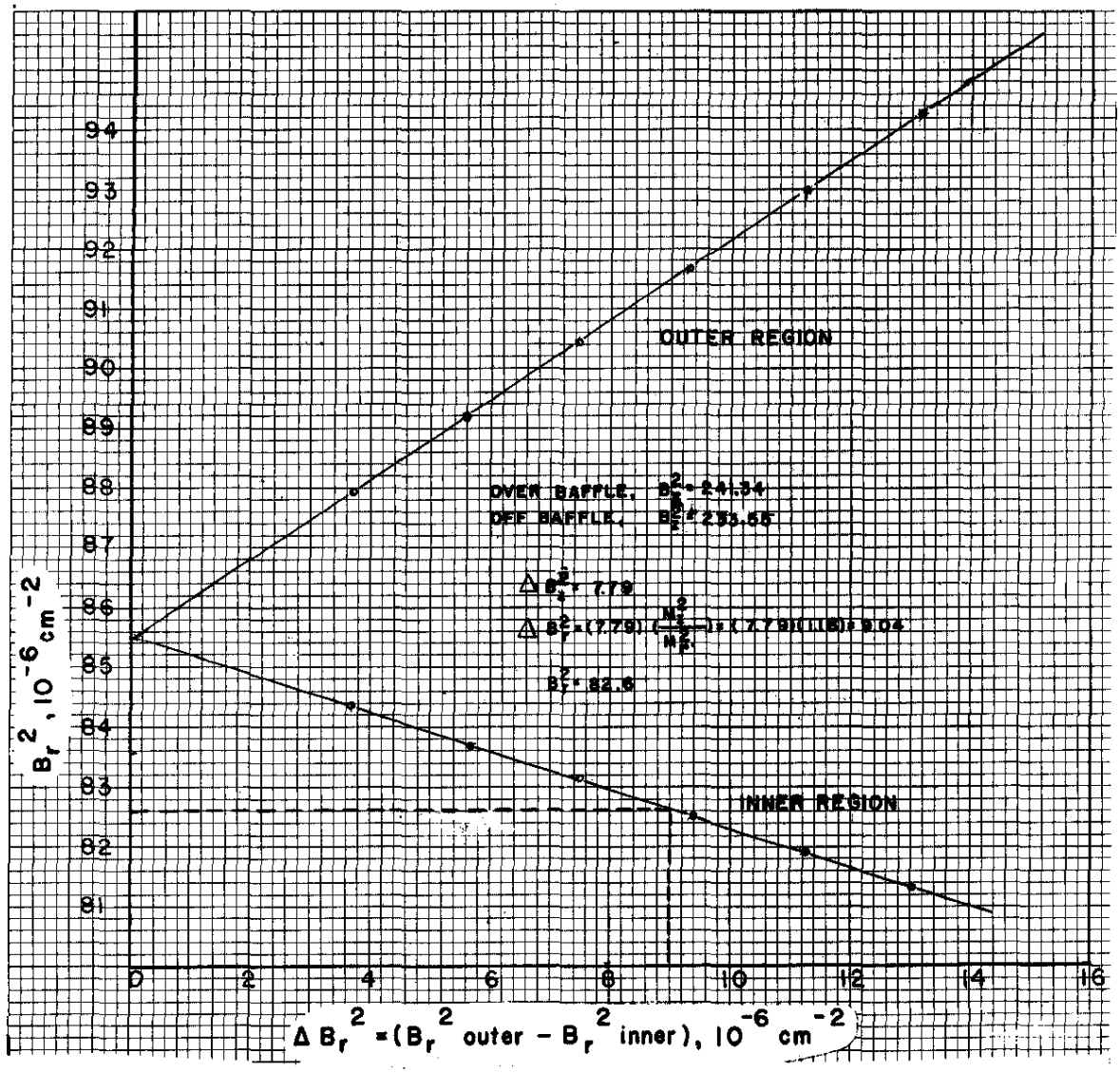

FIG. 17 TWO REGION CODE RESULTS

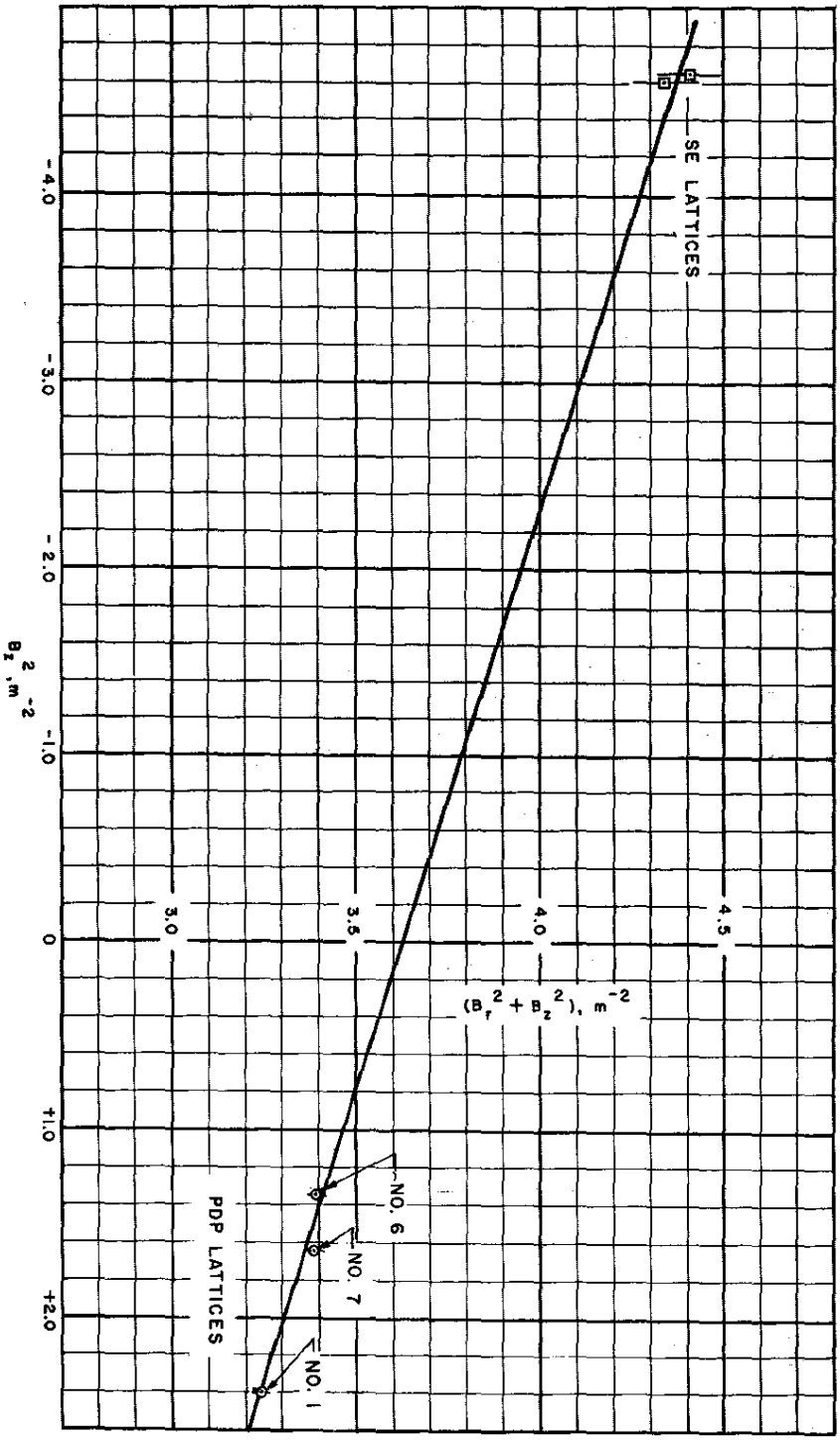

FIG. 18 ANISOTROPHY EL-4 LATTICE

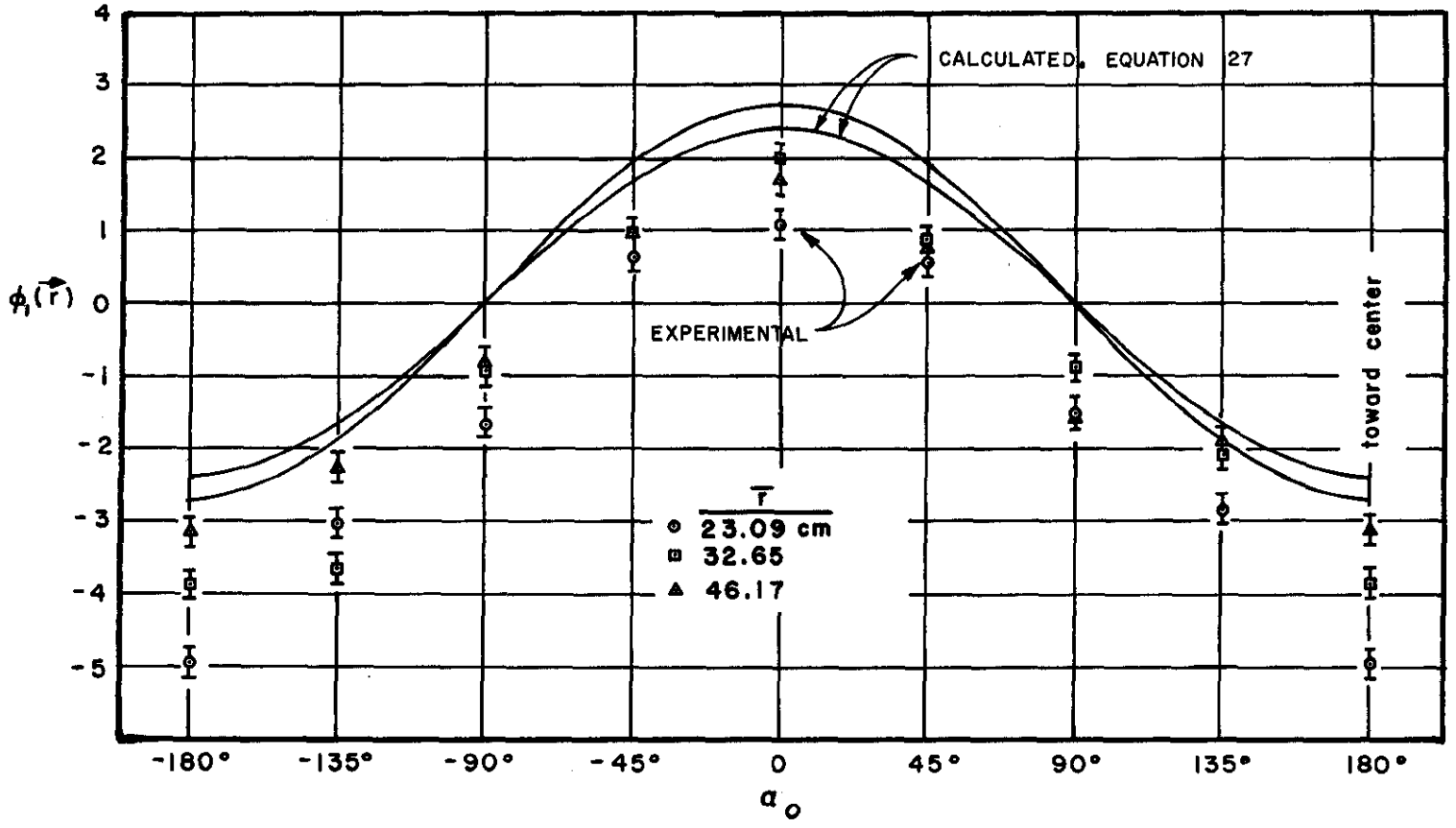

FIG. 19 FUEL CENTERED LATTICE, PALMEDO-BENOIST METHOD FOR D_r/D_m

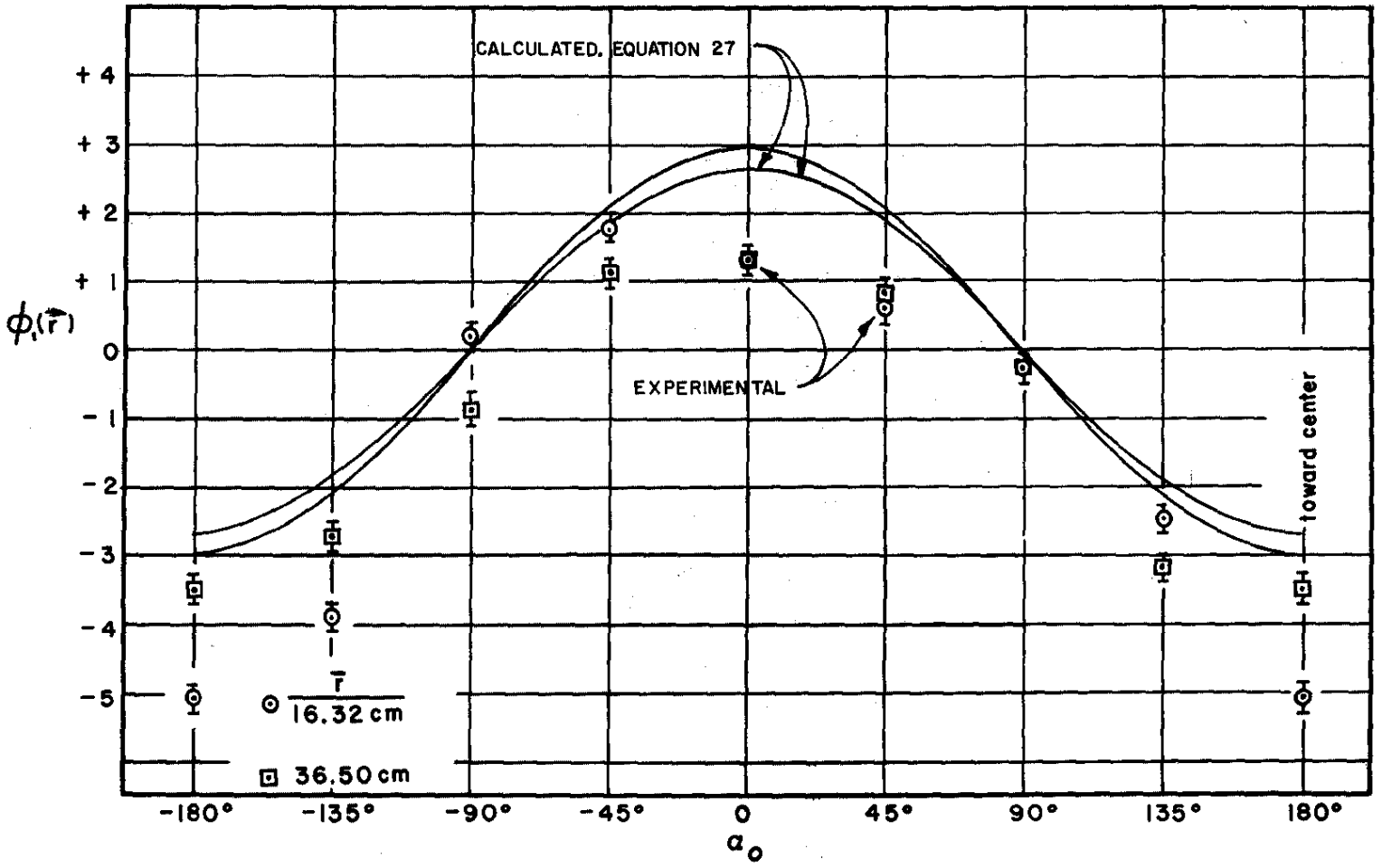

FIG. 20 MODERATOR CENTERED LATTICE, PALMEDO-BENOIST METHOD FOR D_r/D_m

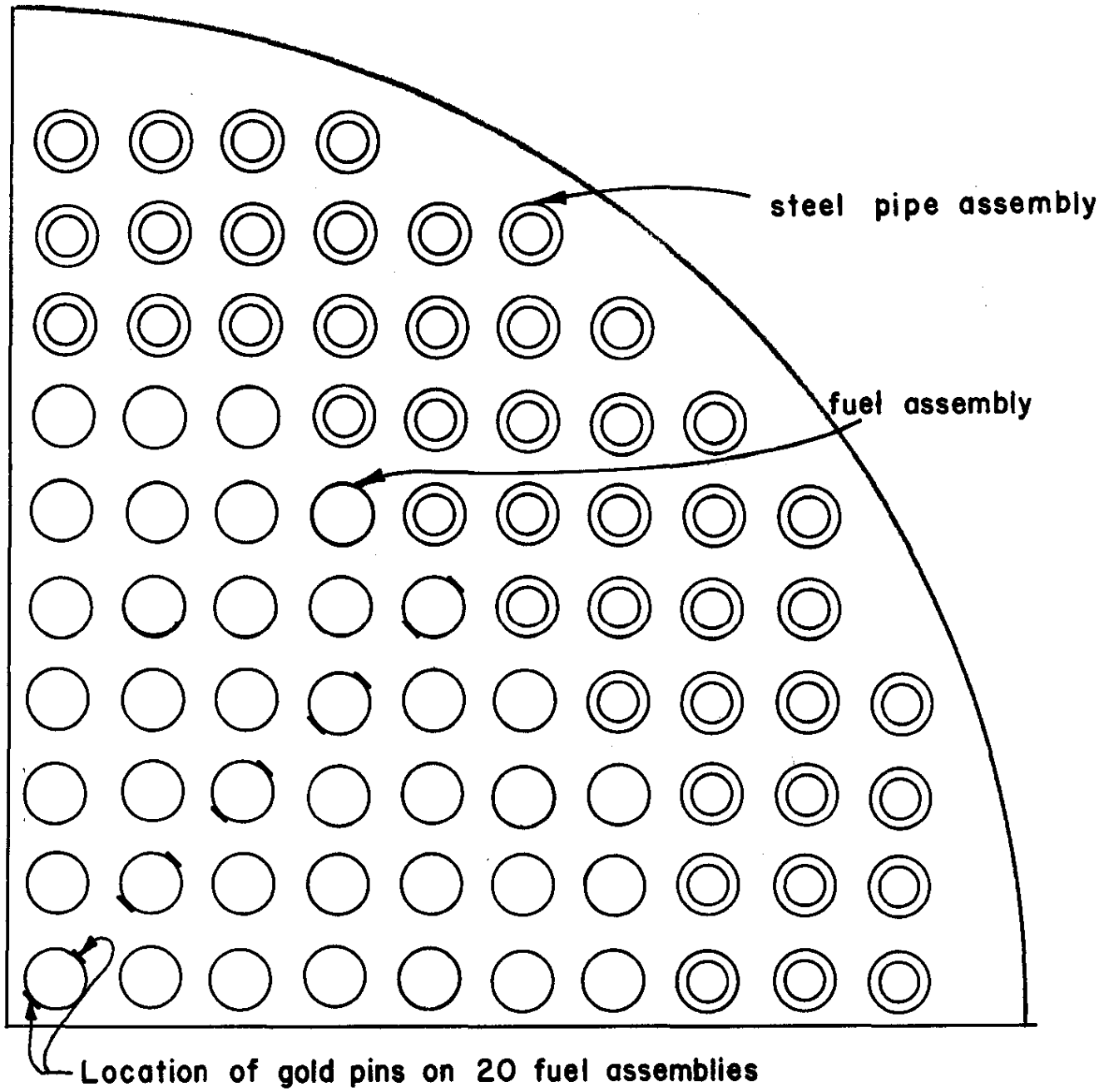

FIG. 21 PALMEDO-BENOIST MEASUREMENT OF D_r/D_m IN PDP

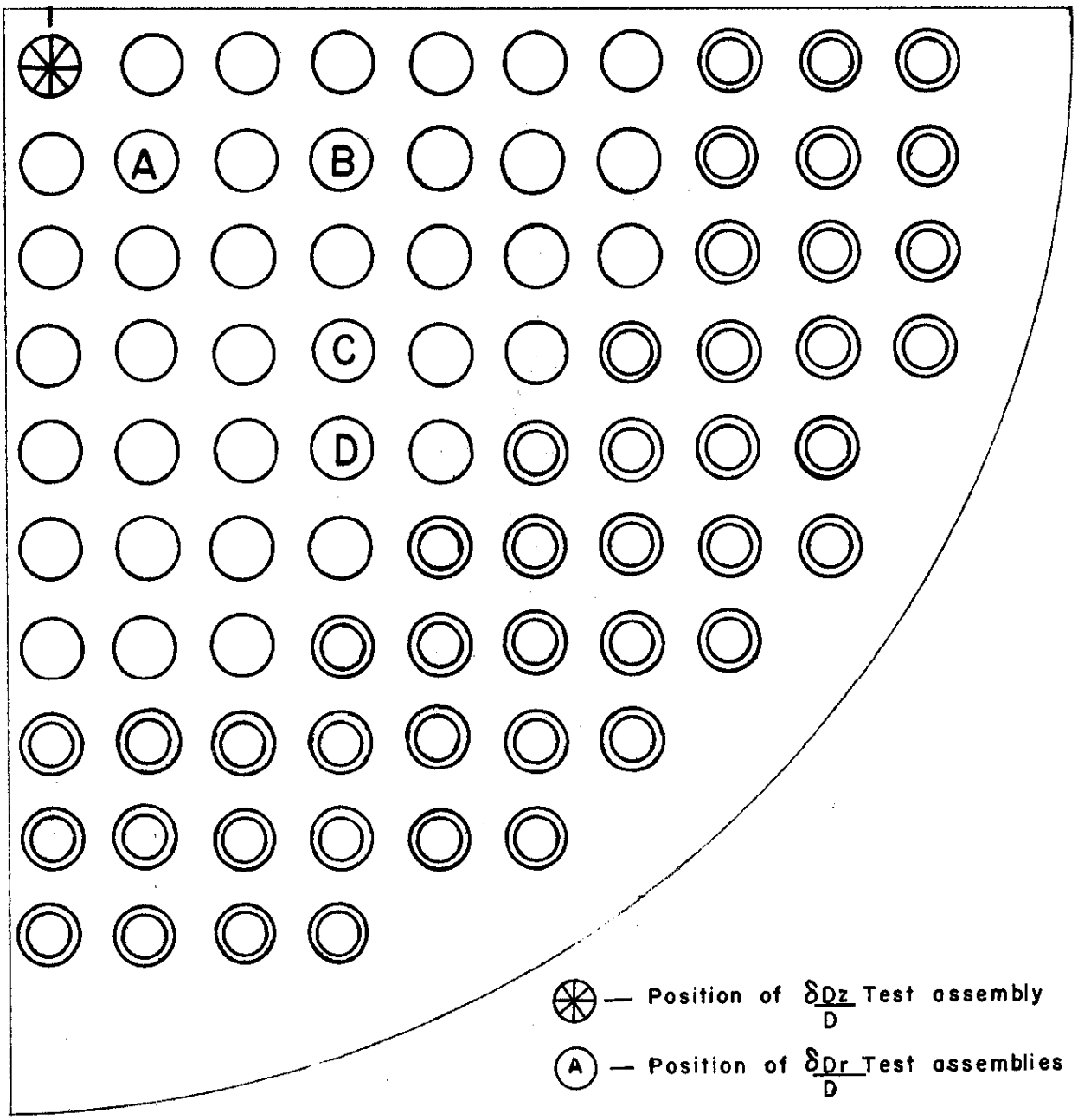

FIG. 22 TEST FUEL POSITIONS δ D/D MEASUREMENTS IN PDP

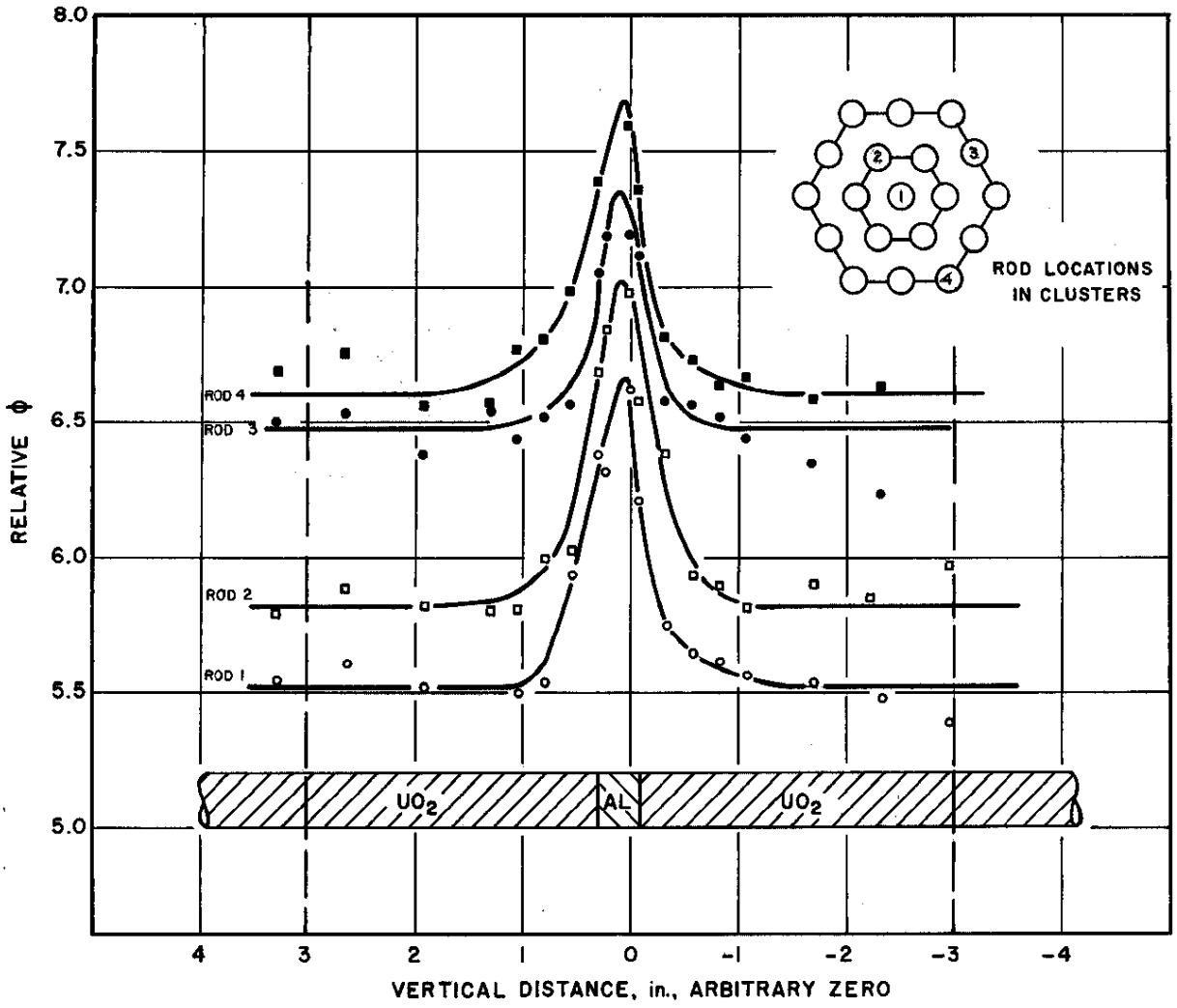

FIG. 23 CORRECTED FOIL ACTIVATIONS ACROSS FUEL GAP

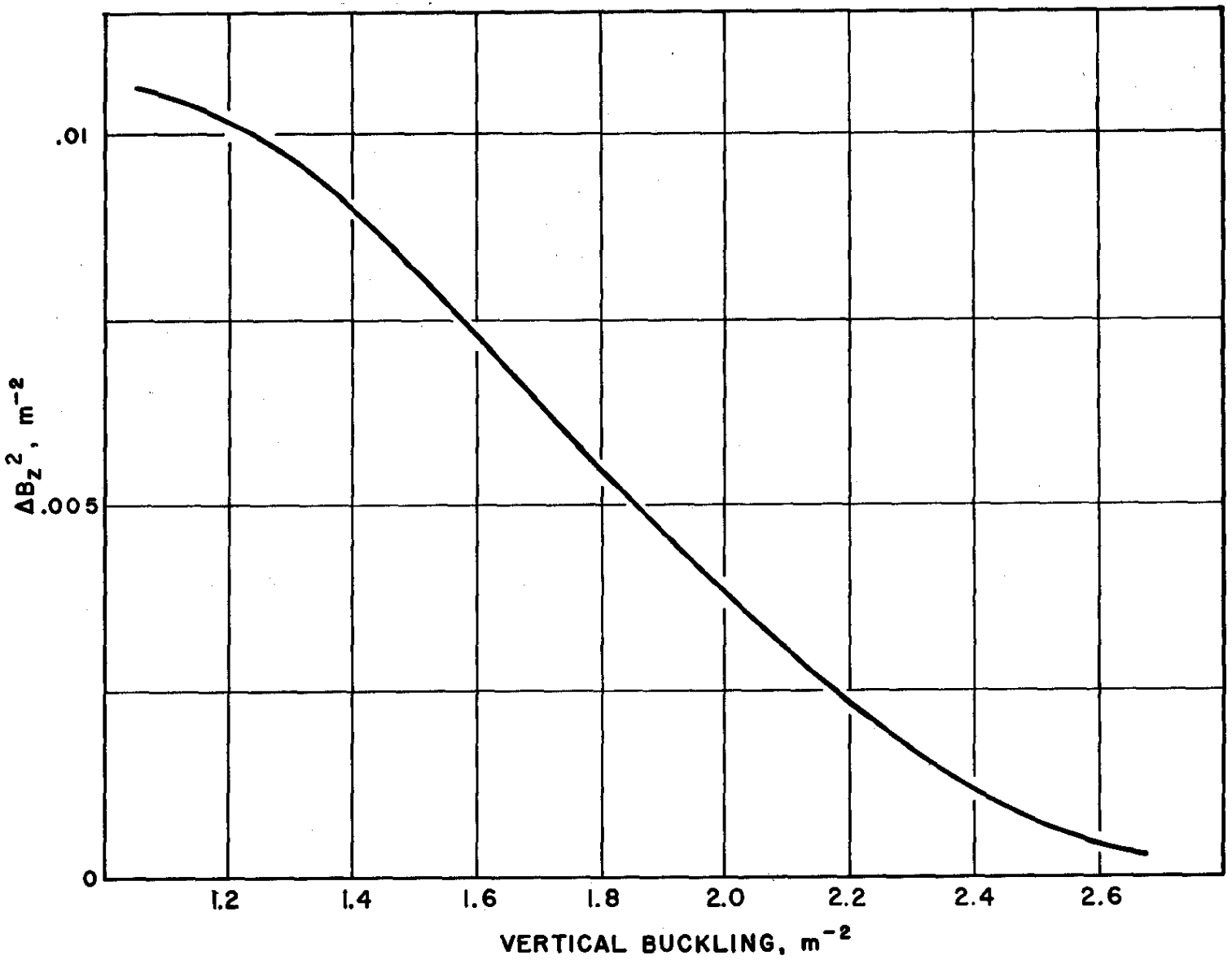

FIG. 24 ΔB_z^2 DUE TO FUEL GAP VS VERTICAL BUCKLING

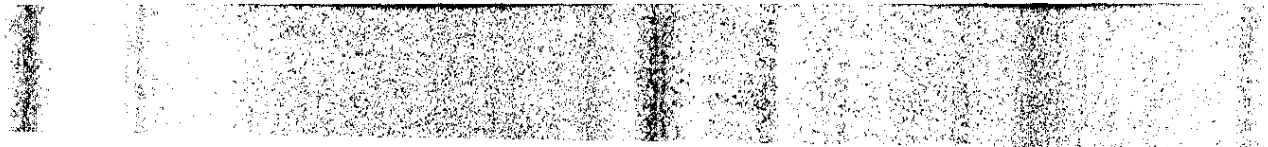

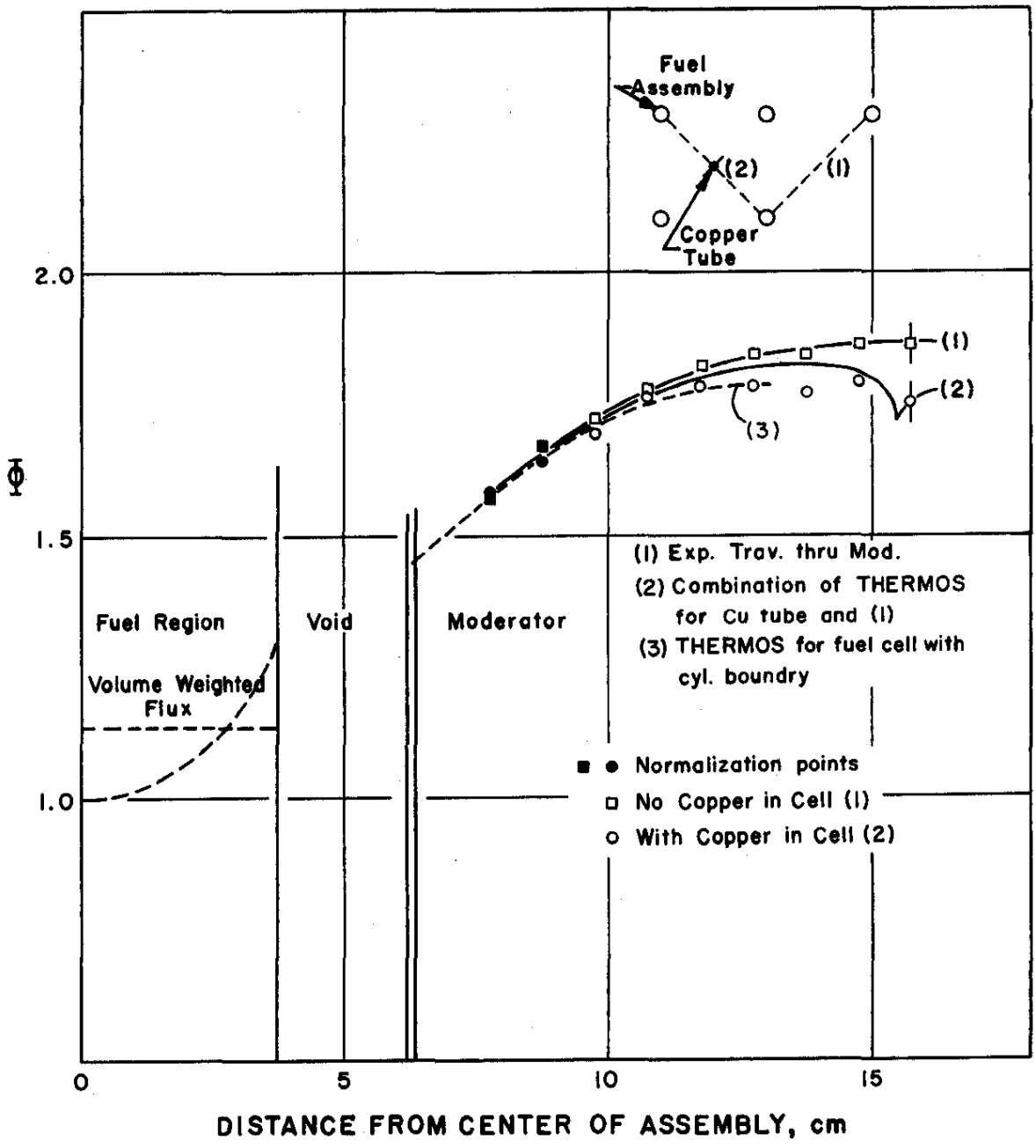

FIG. 25 CELL TRAVERSE WITH COPPER WIRE

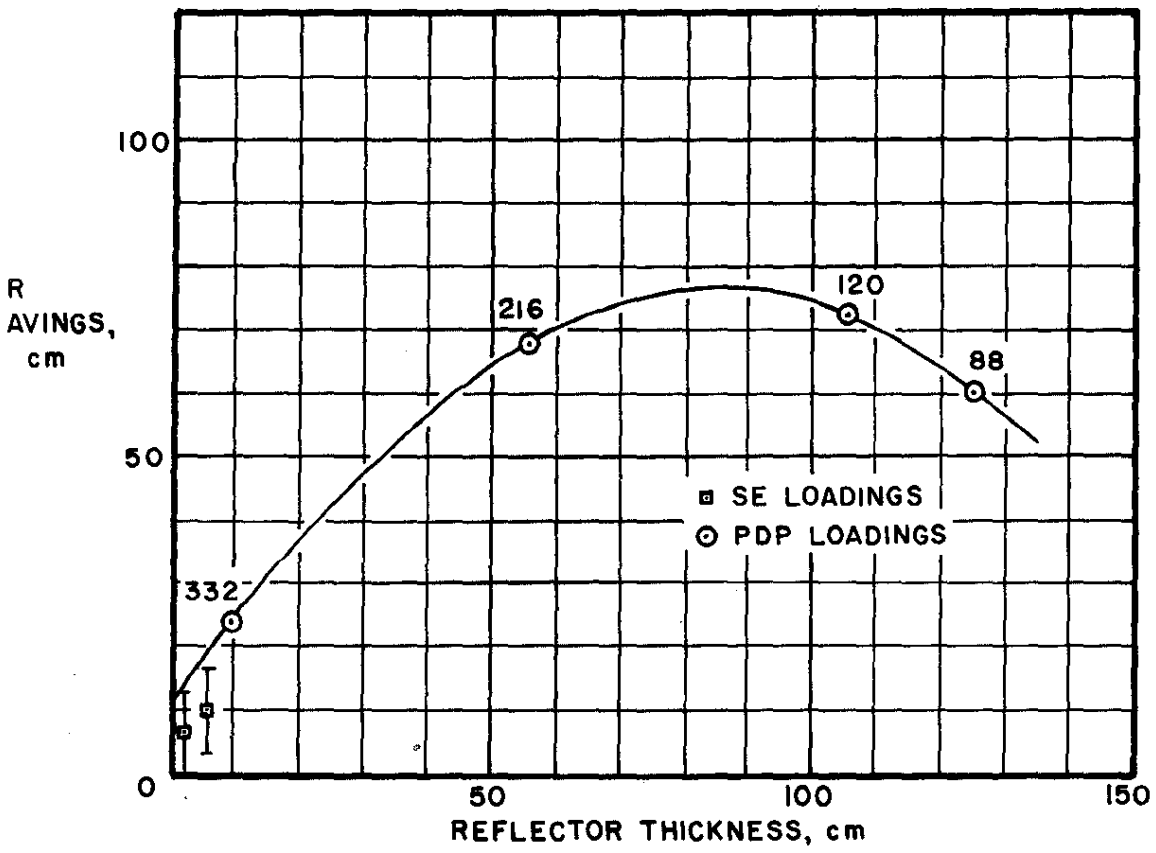

FIG. 26 REFLECTOR SAVINGS